

## **Chapter 5**

# **Magnetic Interaction**

**in**

**$\text{Fe}_x\text{Sb}_{1-x-y}\text{Se}_y$  system**

## 5.1 Introduction:

Semiconducting compounds and alloys whose lattices are made in part of substitutional magnetic atoms are known as Semimagnetic semiconductors (SMSC) or Diluted Magnetic Semiconductors (DMS). Mixed crystals like  $\text{Pb}_{1-x}\text{Gd}_x\text{Te}$ ,  $\text{Cd}_{1-x}\text{Mn}_x\text{Te}$ ,  $\text{Hg}_{1-x}\text{Fe}_x\text{Se}$ ,  $\text{Zn}_{1-x}\text{Mn}_x\text{Te}$  are some of the examples of these types of systems. These materials have some unique properties, which enhances their potential for use in wide range of opto-electronic devices (1,2,3,4,5).

These diluted magnetic semiconductors exhibit existence of magnetic phenomenon with simple crystallographic and band structure. They possess typical optical and transport properties. There exists the possibility of controlled doping of magnetic ion concentration in these systems. The band gap and lattice parameters can be tuned by changing the concentration of magnetic impurities. The Fe based SMSC were reviewed in (6).

The presence of substituted magnetic ions in the DMS results in magnetic properties, which distinguish them from ordinary semiconductors. In contrast to other normal magnetic semiconductors for which the application of an external magnetic field doesn't produce a marked response by magnetic ions, the magnetic ions in DMS do respond to applied magnetic field and change the energy band and

impurity level parameters. The DMS most widely studied are the  $A^{II}-B^{IV}$ ,  $A^{IV}-B^{VI}$  and  $A^{III}-B^V$  type in which magnetic ions like Mn, Co and Fe are introduced as impurities. Magnetic properties of SMSC are of interest as they depend on the type of magnetic ion introduced in the matrix. These transition metals and rare earth magnetic ions form well localised magnetic moments in the semiconducting matrix (1,2,6,7). The magnetic moment of Mn is purely due to spin with out any orbital moment contribution. But Fe has a non vanishing orbital momentum which results in Van Vleck type of Paramagnetism.

All the II-VI, III-V or IV-VI compounds have both the components (transition metals and Chalcogenides) as part of the lattice in which the magnetic ion (Fe,Mn,Cr etc) is introduced. Thus normal Semimagnetic semiconducting systems contain a full unit of the chalcogen per formula. In none of the studies so far the B site proportion of the chalcogen has been varied. In all the experiments the magnetic ion doping was done only at the A site leaving the full formula unit at B. It will be interesting to study the effect of varying the chalcogen concentration in the III-V Sb-Se system doped with magnetic ion Fe. The present study deals with the variation of the concentration of the chalcogen in the small concentration range.

The general formula of the present system is  $Fe_xSb_{1-x-y}Se_y$  where the concentration of Se is varied for different concentrations of Fe. Three concentrations of X (Fe) are studied viz. 0.002, 0.004 and 0.008. For X (Fe) = 0.002 (series 1) the three concentrations of Se viz. Y = 0.004, 0.016 and 0.048 and for X = 0.008 (series 3) the Se concentrations and Y = 0.004, 0.008 and 0.016 were studied. For X (Fe) = 0.004 only one concentration of Se (Y = 0.004) was studied (series 2).

## 5.2 Sample Preparation:

The desired quantities of the material of 99.99 % purity were taken to make the  $Fe_xSb_{1-x-y}Se_y$  samples. All the present samples were made with enriched Fe-57 metal sheet or powder as the concentration of Fe is quite small. The samples were sealed in a small quartz tube at very high vacuum  $>10^{-5}$  torr and they were then heat treated in oxy-butane flame. The samples were melted and kept in melting condition for 5-10 minutes. They were then cooled to room temperature, and were re melted. This process was repeated several times and in the final cycle every sample was quenched in water from the melt condition. Each of the samples was obtained as small globules.

### 5.3 Experimental:

All the present samples were studied by Mossbauer technique. A constant acceleration Mossbauer spectrometer was used for the study. The Fe-Sb-Se samples were powdered and approximately 100mg. of each of the samples was taken to make the Mossbauer absorbers. The samples were evenly distributed on a one mm thin sheet of paper of 1.2 cm diameter. Before each run of the spectra the velocity calibration was checked and recorded. A typical calibration spectrum of natural Fe is shown in Fig 5.1 A. The calibration was also varied according to the need of the sample. All the spectra were recorded at room temperature by a 50 mCi source in Rh matrix. The line width of the spectrometer is 0.28 mm/sec.

### 5.4 Results and Discussion:

The Mossbauer parameters of the samples at room temperature are given in Table 5.1, 5.2 and 5.3. The table 5.1 gives the results of the first series ( $X=0.002$ ,  $Y= 0.004, 0.016$  and  $0.048$ ). For comparison the sample with formula  $Fe_xSb_{1-x}$  where  $X=0.002$  is also given in the table. In table 5.2 along with  $X=0.004$  and  $Y=0.004$  also the values of  $X=0.002$  and  $0.008$  for  $Y=0.004$  are given for comparison. The Table 5.3 gives the parameters of the third series ( $X=0.008$ ,  $Y= 0.004, 0.008$  and  $0.016$ ). The experimental errors are given in parenthesis. The

FIG. 5.1 A

Calibration Mossbauer Spectrum of Natural Fe

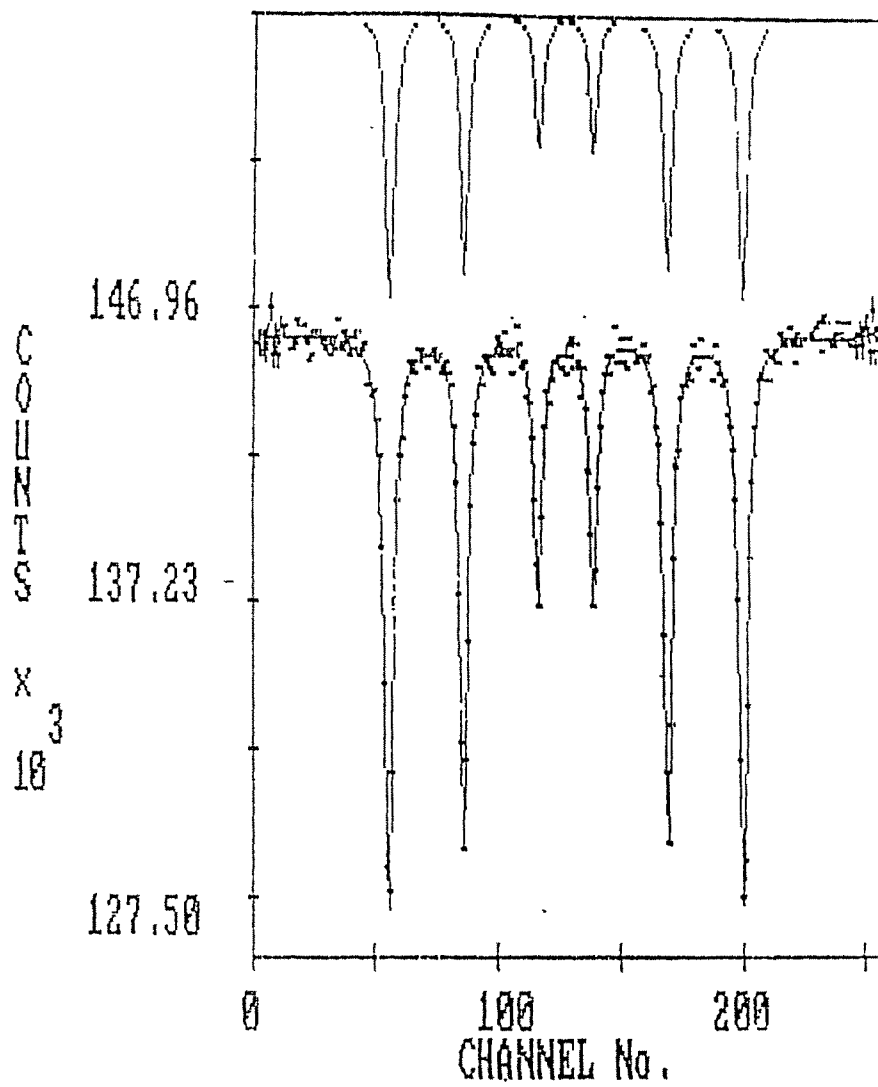


Table 5.1

## Series I

 $\text{Fe}_x\text{Sb}_{1-x-y}\text{Se}_y$  for  $X = 0.002$ ,  $Y = 0.004, 0.016$  and  $0.048$ 

Sample	Value of field (KOe)		QS Mm/sec	Isomer Shift (mm/sec)			Area		
	A	B	C	A	B	C	A	B	C
X=0.002	311.5 (2.4)	-	-	-0.76 (0.03)	-	-	100	-	-
X = 0.002 Y = 0.004	309.2 (1.5)	269.9 (1.5)	-	-0.78 (0.02)	-0.70 (0.02)	-	.462	.538	-
X = 0.002 Y = 0.016	289.7 (1.2)	263.8 (1.2)	-	-0.74 (0.02)	-0.69 (0.02)	-	.506	.494	-
X = 0.002 Y = 0.048	279.7 (1.6)	251.8 (1.6)	0.51 (0.02)	-0.76 (0.02)	-0.68 (0.02)	-0.28 (0.02)	.522	.361	.117

Table 5.2

## Series II

 $\text{Fe}_x\text{Sb}_{1-x-y}\text{Se}_y$  for  $Y = 0.004$ ,  $X = 0.002, 0.004$  and  $0.008$ 

Sample	Value of field		QS mm/sec	Isomer Shift (mm/sec)			Area		
	A	B		A	B	C	A	B	C
X = 0.002 Y = 0.004	309.2 (1.5)	269.9 (1.5)	-	-0.78 (0.02)	-0.70 (0.02)	-	.462	.538	-
X = 0.004 Y = 0.004	308.2 (1.6)	254.8 (1.6)	1.26 (.02)	-0.69 (0.02)	-0.69 (0.02)	-0.44 (0.02)	.452	.362	.186
X = 0.008 Y = 0.004	308.7 (2.6)	272.5 (2.6)	1.26 (0.02)	-0.66 (0.02)	-0.53 (0.02)	-0.44 (0.02)	.110	.156	.734

Table 5.3

## Series III

 $\text{Fe}_x\text{Sb}_{1-x-y}\text{Se}_y$  for  $X = 0.008$ ,  $Y = 0.004, 0.08$  and  $0.016$ 

Sample	Value of field in (KOe)		QS Mm/sec	Isomer Shift (mm/sec)			Area		
	A	B	C	A	B	C	A	B	C
X = 0.008	308.7	272.5	1.26	-0.66	-0.53	-0.44	.110	.156	.734
Y = 0.004	(2.6)	(2.6)	(0.02)	(0.02)	(0.02)	(0.02)			
X = 0.008	301.1	244.4	1.26	-0.69	-0.66	-0.47	.169	.293	.544
Y = 0.008	(1.6)	(1.6)	(0.02)	(0.02)	(0.02)	(0.02)			
X = 0.008	250.5	194.0	1.29	-0.69	-0.55	-0.43	.581	.337	.117
Y = 0.016	(1.6)	(1.6)	(0.02)	(0.02)	(0.02)	(0.02)			

isomer shifts are with respect to Natural Fe. All the Mossbauer spectra were least square fitted with a computer program.

In the case of first series (where  $X=0.002$ ) the Mossbauer spectra could be fitted with two magnetic sextet (A and B) for  $Y=0.004$  and  $0.016$ . In case of  $Y=0.048$  the spectrum could be fitted with two sextet and a doublet ( C ). As Se concentration is varied from  $Y = 0.004$  to  $0.048$  the field A is found to change from  $309.2$  KOe to  $279.7$  KOe and field B varies from  $270$  KOe to  $252$  KOe. For the three sets, the value of Isomer Shift (IS)  $\sim -0.76$  mm/sec for A site and  $-0.70$  mm/sec for B site. The value of  $QS = 0.51$ mm/sec for the doublet for the  $X=0.002$  and  $Y=0.048$ .

The value of magnetic fields for the second series  $X=0.004$  and  $Y=0.004$  are  $\sim 308$  KOe (A site) and  $\sim 255$ KOe (B site) respectively. The value of Quadrupole doublet is  $1.26 \pm 0.02$  mm/sec.

Similarly for the Mossbauer spectra of the third series i.e.  $X=0.008$  and  $Y=0.004, 0.008$  and  $0.016$  we could fit all the spectra with two sextet (A and B) and a quadrupole doublet ( C ). The value of magnetic field (A) in these cases varies from  $\sim 308$  KOe to  $250$  KOe. The magnetic field B for Se values ranging from  $0.004$  to  $0.016$  is found to vary from  $\sim 272$  KOe to  $\sim 194$  KOe. In all the cases the value of Quadrupole splitting  $\sim 1.26 \pm 0.02$  mm/sec.

Fig. 5.1.1

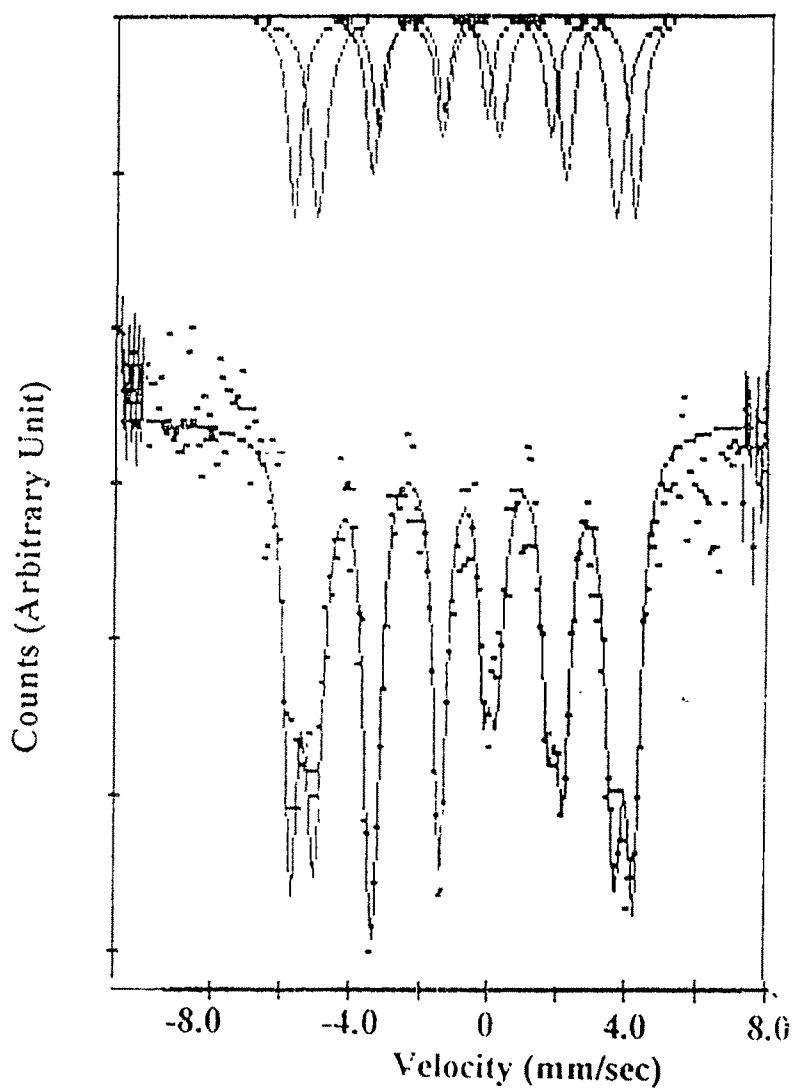
 $\text{Fe}_x\text{Sb}_{1-x-y}\text{Se}_y$  (For  $X = 0.002$ ,  $Y = 0.004$ )

Fig. 5.1.2

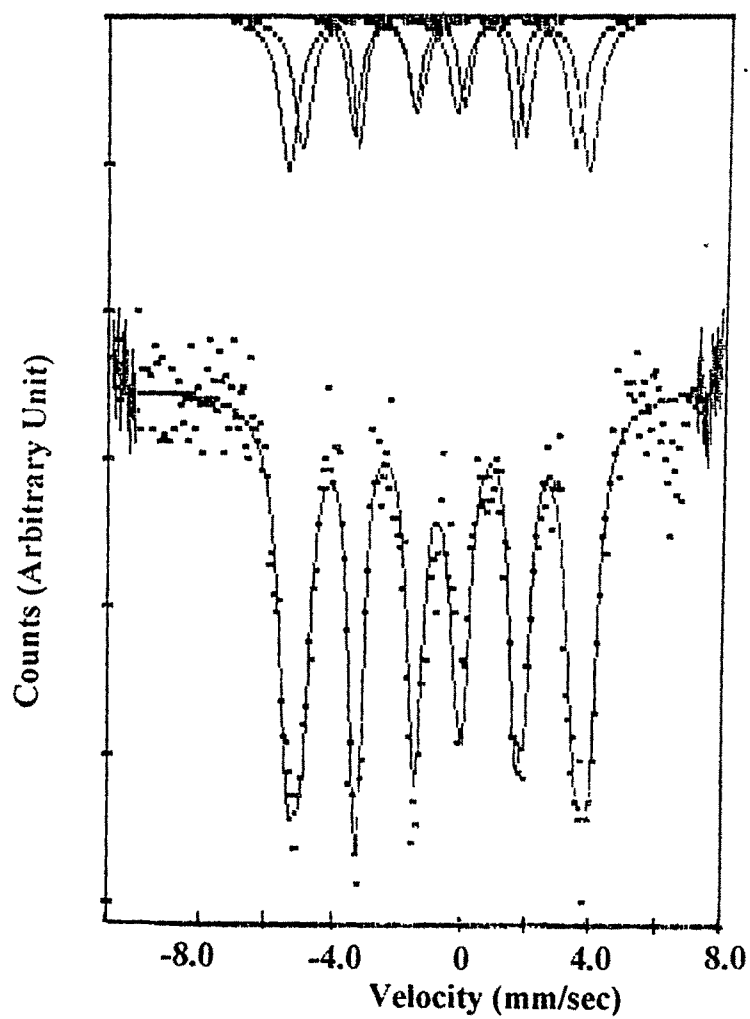
 $\text{Fe}_x\text{Sb}_{1-x-y}\text{Se}_y$  (For  $X = 0.002$ ,  $Y = 0.016$ )

Fig. 5.1.3

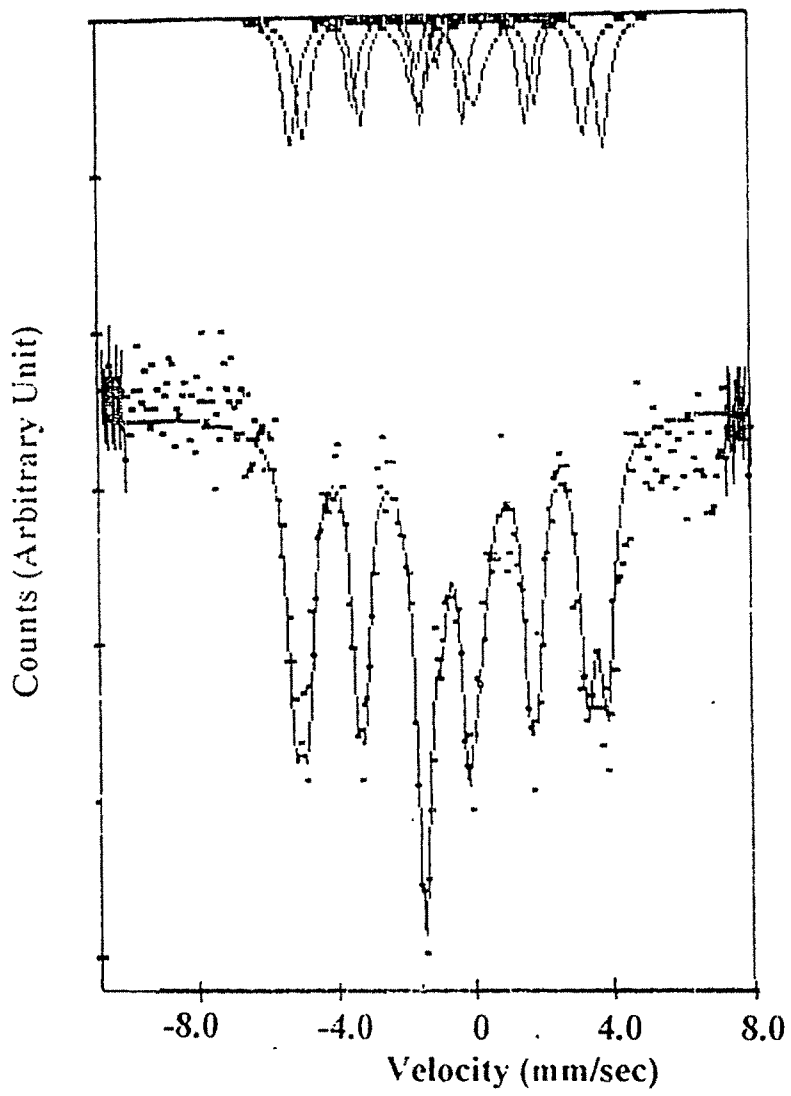
 $\text{Fe}_x\text{Sb}_{1-x-y}\text{Se}_y$  (For  $X = 0.002$ ,  $Y = 0.048$ )

Fig. 5.1.4

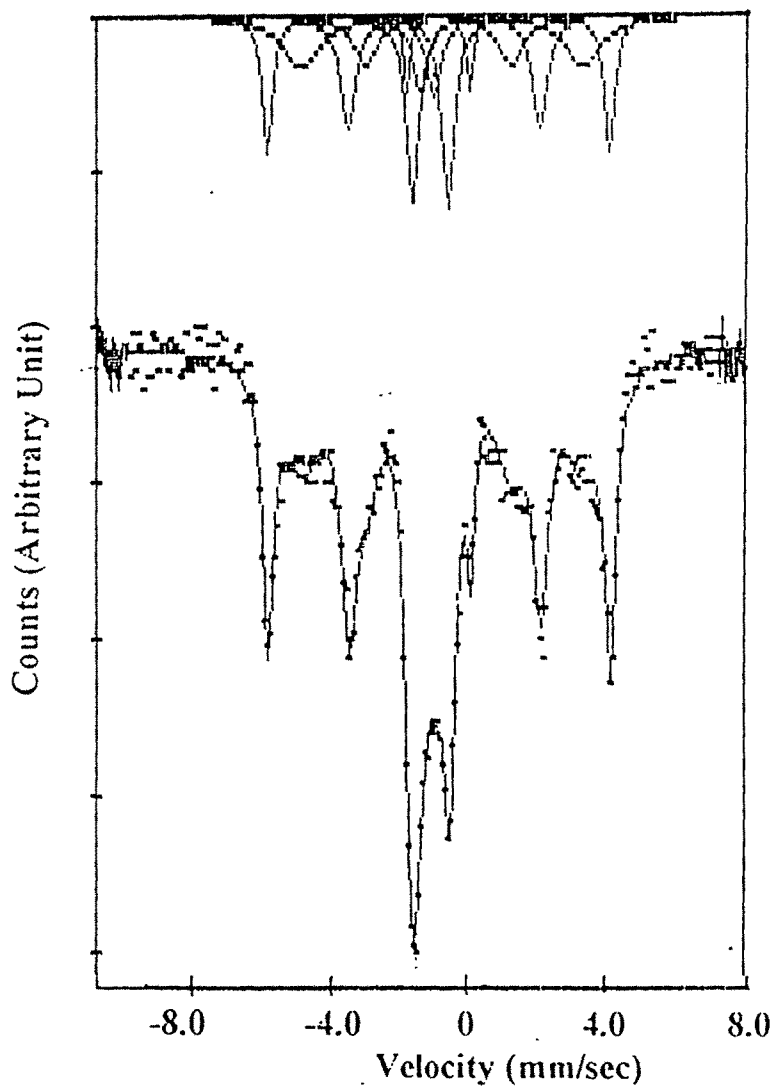
 $\text{Fe}_x\text{Sb}_{1-x-y}\text{Se}_y$  (For  $X = 0.004$ ,  $Y = 0.004$ )

Fig. 5.1.5

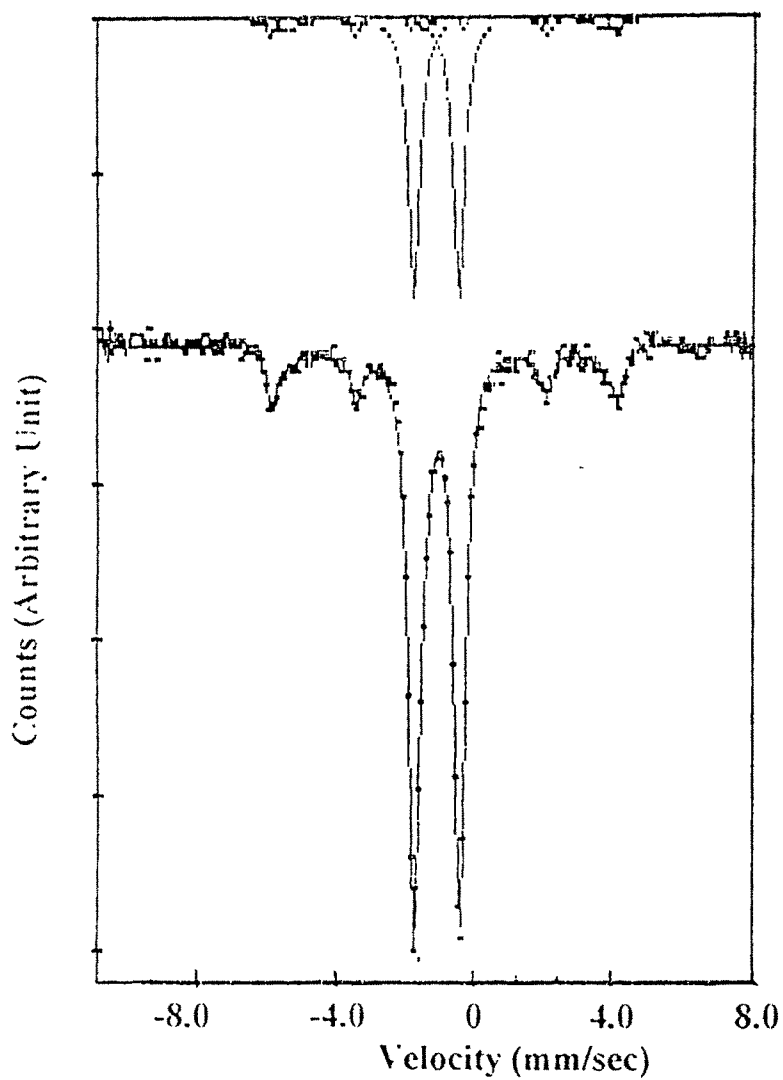
 $\text{Fe}_x\text{Sb}_{1-x-y}\text{Se}_y$  (For  $X = 0.008$ ,  $Y = 0.004$ )

Fig. 5.1.6

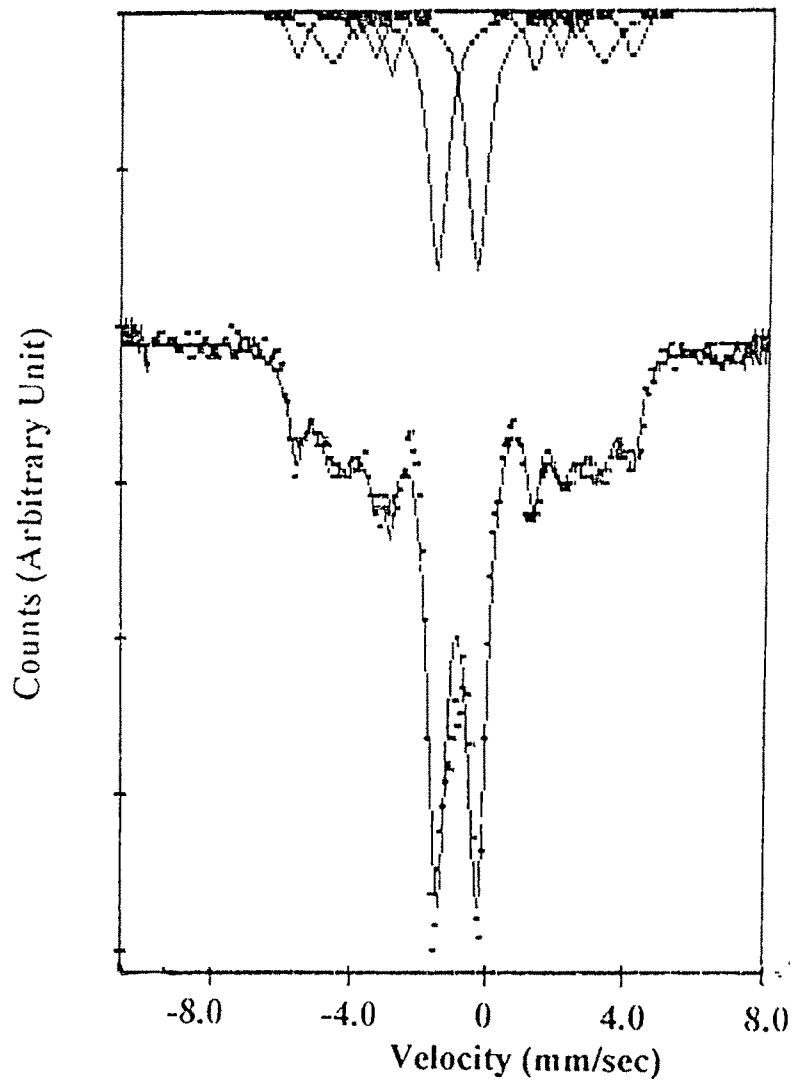
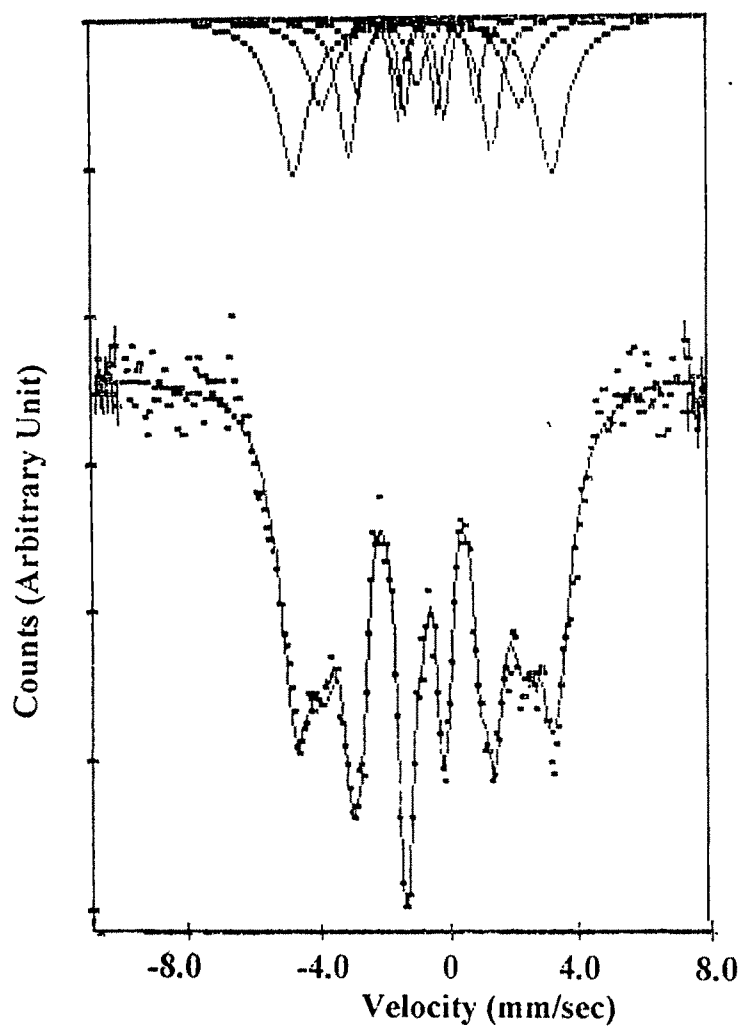
 $\text{Fe}_x\text{Sb}_{1-x-y}\text{Se}_y$  (For  $X = 0.008$ ,  $Y = 0.008$ )

Fig. 5.1.7

 $\text{Fe}_x\text{Sb}_{1-x-y}\text{Se}_y$  (For  $X = 0.008$ ,  $Y = 0.016$ )

Mossbauer spectra of all the three series are given from Fig. 5.1.1 to 5.1.7. As explained in chapter four for samples free from Se and for Fe concentration of  $0.005 \leq X < 0.1$ , QS of  $1.28 \pm 0.01$  mm/sec was observed which corresponds to  $\text{FeSb}_2$  formation. For higher concentration of Fe in Sb, the formation of FeSb also takes place, which shows a narrow quadrupole splitting of  $0.29 \pm 0.01$  mm/sec. It was also mentioned that for Fe :  $X \leq 0.0025$ , a magnetic field of  $311 \pm 2.1$  KOe was observed.

The introduction of Se ( $Y = 0.004$ ) in the Fe ( $X = 0.002$ ) Sb system resulted in Fe showing two magnetic sites. This indicates that Fe has two inequivalent surroundings unlike the Fe (0.002) Sb case discussed in Chapter 4 where Fe was in a unique field of  $\sim 310$  KOe.

Further it can be noted that all the IS values are negative ( $\sim -0.76$  mm/sec) in case of Fe-Sb-Se systems like in the FeSb ( $X \leq 0.002$ ) system which is also negative ( $\sim -0.76$  mm/sec). Hence Fe can be seen to be in predominantly  $4+$  charge state or higher.

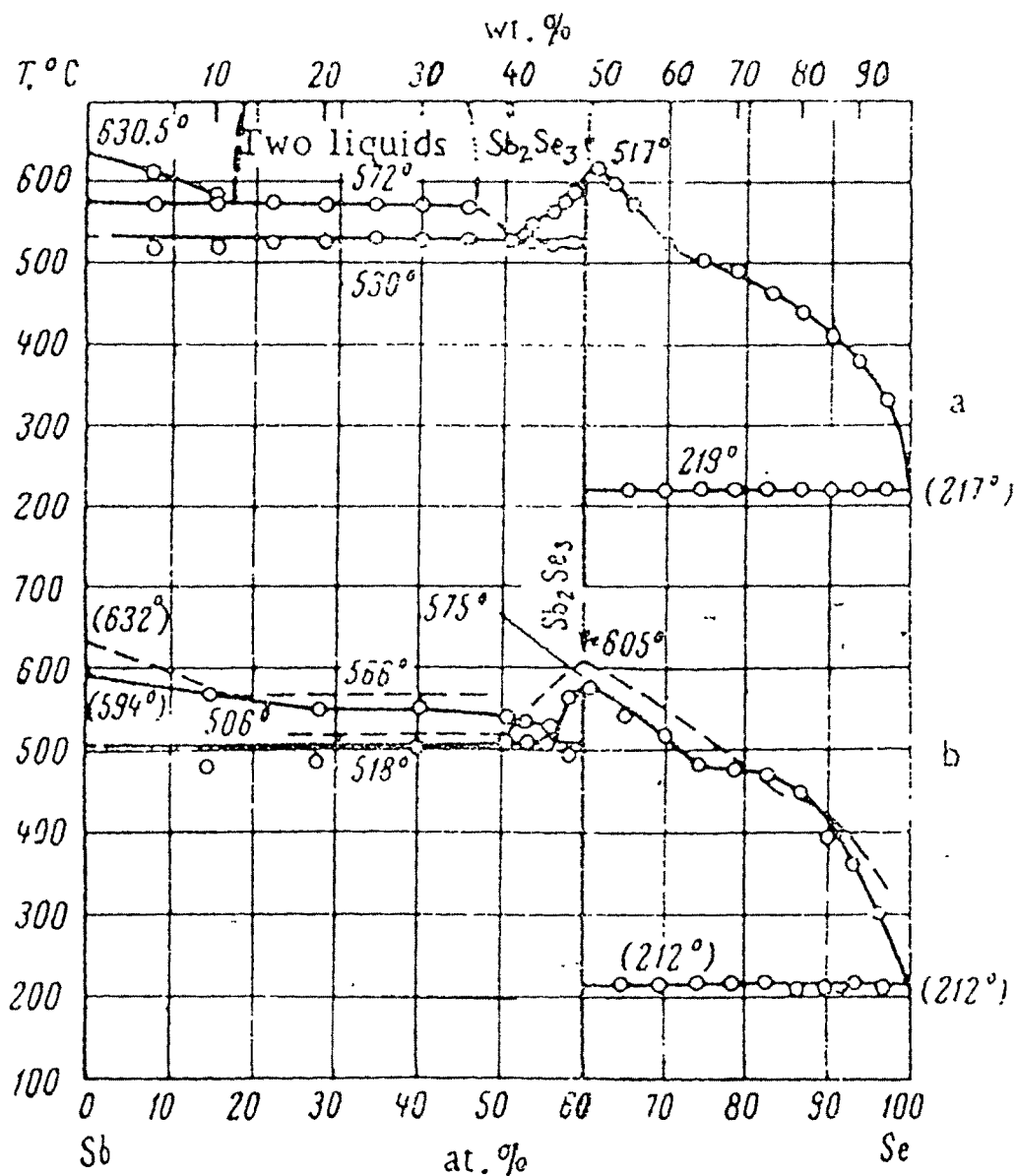
When the concentration of Se is increased to ( $Y = 0.016, 0.048$ ) the value of the field at both the sites decreased. There is not much change in the value of

the Isomer Shift indicating Fe to be in a predominantly 3+ charge state. For Se ( $Y=0.048$ ) a small quadrupole doublet of  $\sim 0.53$  mm/sec was also observed. This may be ascribed to the compound formation between Sb and Se. As the concentration of Se was more it is likely that Sb and Se might be interacting to form a compound of Sb and Se. From the phase diagram (Fig. 5.1 B) also it can be seen that a compound  $Sb_2Se_3$  exists.

To confirm whether this doublet to Fe in  $Sb_2Se_3$  a sample of  $Sb_2Se_3$  was made. Fe (0.002) was incorporated in this sample to find the interaction of Fe in this compound. The observed spectrum could be fitted with a doublet in the quadrupole splitting of 0.535 mm/sec (Fig. 5.1.8). The IS value is  $\sim -0.37$  mm/sec. This value corresponds to the quadrupole doublet seen for the Fe ( $X=0.002$ ) and Se ( $Y=0.048$ ) sample. This indicates that at higher concentration of Se,  $Sb_2Se_3$  formation is more likely. The value of the isomer shift ( $\sim -0.28$  mm/sec) observed for  $X=0.02$  and  $Y=0.048$  can be compared with that of  $Sb_2Se_3$  compound which is  $-0.37$ . This indicates Fe is in +3 charge state.

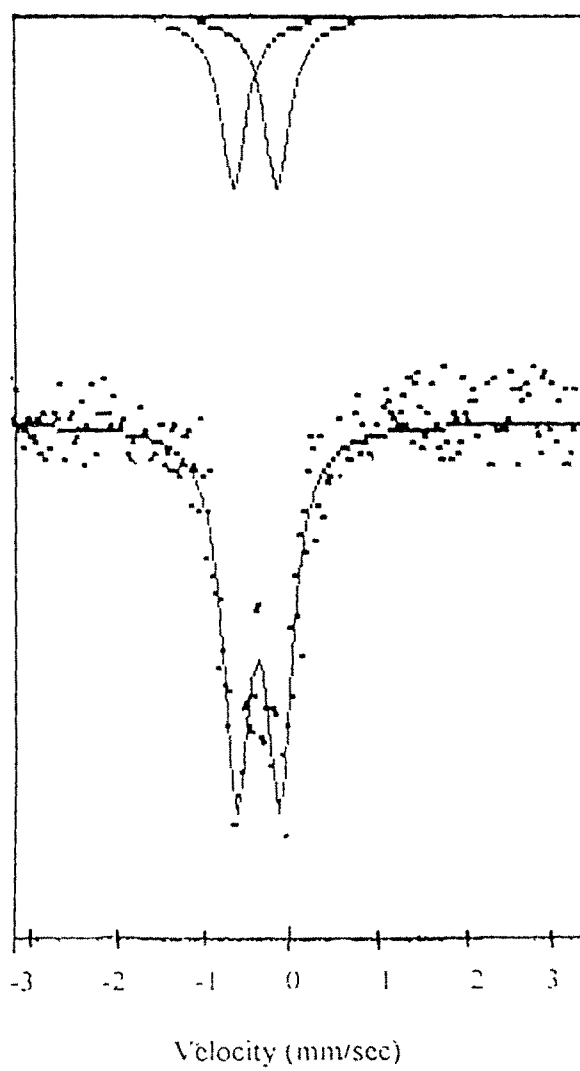
It is also possible that non-magnetic Fe-Se compounds like FeSe,  $FeSe_2$  may form in these systems. However, the isomer shift for these compounds is +ve (8,9) and here they can be ruled out. The observed line width in the case of Fe ( $X=0.002$ ) and Se ( $Y=0.004, 0.016$  and  $0.048$ ) is  $\sim 0.46 \pm 0.02$  mm/sec. The line

Fig. 5.1 B



Phase diagram of Sb - Se system

Fig. 5.1.8

Mossbauer spectrum of  $\text{Fe}_{0.002}(\text{Sb}_2\text{Se}_3)$ 

width of the spectrometer is  $\sim 0.30 \pm 0.02$  mm/sec. This indicates that the observed fields in the cases are unique.

The second series displays the Mossbauer parameters for a constant Se concentration ( $Y=0.004$ ) with the increasing Fe concentration ( $X=0.002, 0.04, 0.008$ ). The higher concentration of Fe ( $X=0.004$  and  $0.008$ ) system could be fitted with two sextets and a doublet. The value of the quadrupole doublet corresponds to value of  $\text{FeSb}_2$ .

It was also found that the value of the magnetic field at both the sites do not change significantly. Thus at a constant Se concentration addition of more Fe only brings the  $\text{FeSb}_2$  compound formation without altering the magnetic interaction much. However, the IS values are found to decrease with increase of Fe content.

To characterize the samples whether they are semiconductors or not FTIR (Fourier Transformed Infra red spectrophotometer) measurements were done for the samples with Fe ( $X=0.002$ ), Se ( $Y=0.016$ ) and Fe ( $X=0.002$ ), Se ( $Y=0.048$ ). In this case fine powder of the samples was taken with KBr in 1:4 ratio. The samples were thoroughly ground and pellets were made. This pellet was used for FTIR absorption measurements. The band gap can be found out by the plot of  $(\alpha h\nu)^2$  and  $h\nu$ . It is found that the band gap values are 0.175 and 0.18 eV

respectively. This shows that the systems become semiconductors when Se is added to Sb. The graph of  $(\alpha h\nu)^2$  and  $h\nu$  is shown in fig. 5.1 C and 5.1 D.

It should be noted that the concentration variation of Fe in Sb revealed (Chapter 4) that for higher Fe concentrations of 0.005, 0.01, 0.05 in Sb there is no magnetic interaction seen at all. Fe is forming  $\text{FeSb}_2$  at these high concentrations of Fe. But the introduction of Se in this system inhibits the formation of  $\text{FeSb}_2$ . Also the introduction of Se resulted in bringing in the magnetic interaction. However it is interesting to note that the increase in Se concentration decreases the field at both the sites.

The third series consists of study of the effect of variation of Se concentration at the high Fe concentration ( $X=0.008$ ). As expected at this higher concentration of Fe the formation of  $\text{FeSb}_2$  compound was observed. In addition, the two magnetic sites seen in the earlier series are also seen here. Further, it is also found that an increase in Se concentration decreases the field as was seen earlier. This decrease in the field is as sharp as in the series with low concentration of Fe ( $X=0.002$ ) i.e. the first series. This indicates that addition of Se is having a negative effect on the field even though it is bring in magnetic interaction at higher concentrations of Fe.

Fig. 5.1 C

Plot of  $(\alpha h\nu)^2$  vs  $h\nu$  for  $\text{Fe}_x\text{Sb}_{1-x}\text{Se}_y$  for  $X=0.0002$  and  $Y=0.016$

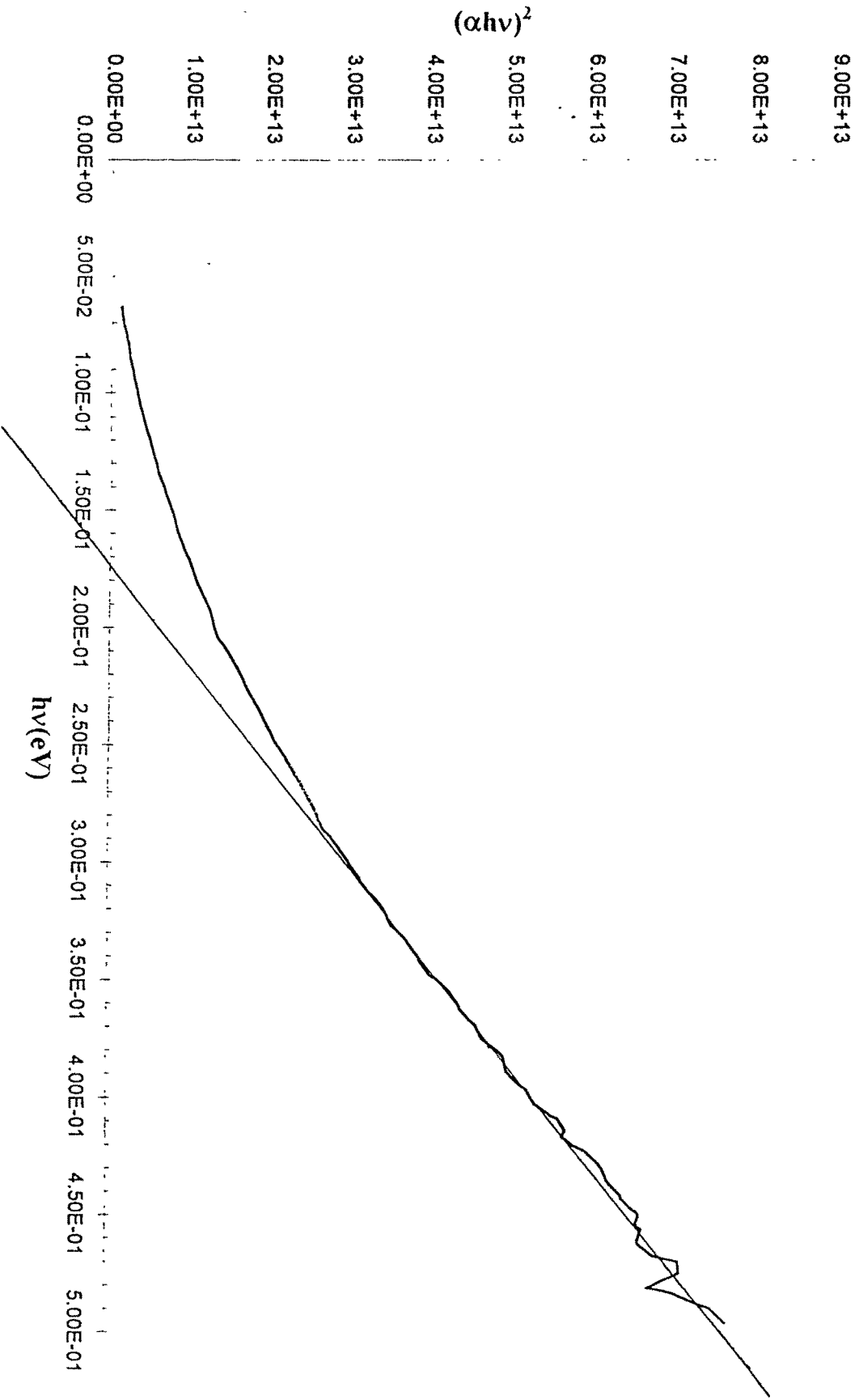
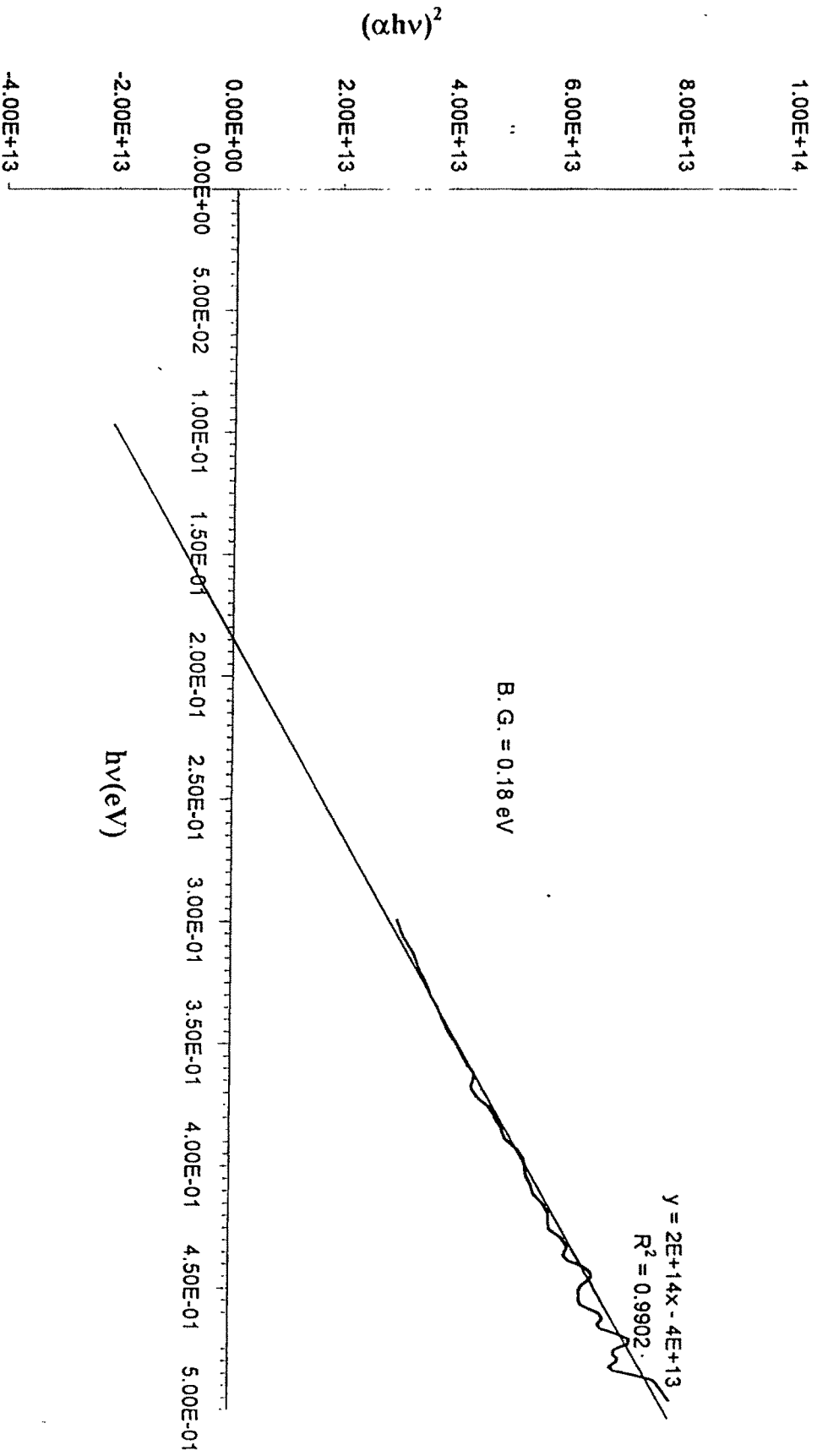


Fig. 5.1 D

Plot of  $(\alpha h\nu)^2$  vs  $h\nu$  for  $\text{Fe}_x\text{Sb}_{1-x}\text{Se}_y$  for  $X=0.0002$  and  $Y=0.048$

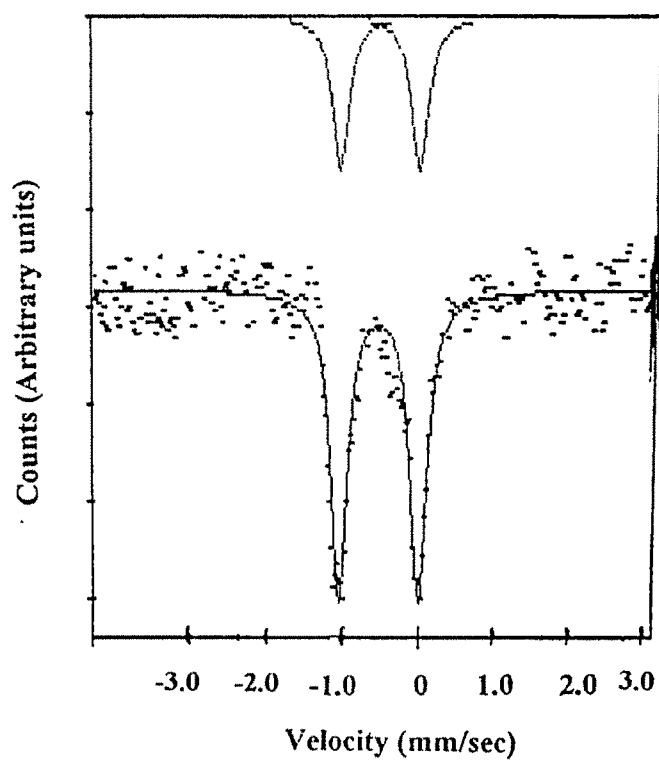


To find out whether Fe exhibits a magnetic interaction at very high concentration of Fe a sample with  $X=0.05$  and  $Y=0.025$  was prepared. This sample showed no magnetic interaction. This spectrum could be fitted with only a doublet and the value of the QS  $1.28 \pm 0.01$  indicated that  $\text{FeSb}_2$  formation has taken place. Thus the presence of Se has been found to have no effect on the  $\text{FeSb}_2$  formation. The Mossbauer spectrum of this sample is given in Fig. 5.1.8.

Thus it shows that at high concentration of Fe,  $\text{FeSb}_2$  formation is most likely even in the presence of Se. As mentioned before that for low Fe concentration and high concentration of Se,  $\text{Sb}_2\text{Se}_3$  compound formation takes place. At high concentration of Fe and low concentration of Se,  $\text{FeSb}_2$  formation is more prominent.

The observed magnetic fields can be understood by considering the following possibilities. The first possibility is the formation of clusters of Fe. Hence to find the presence of clusters of Fe in these systems Neutron depolarisation study was done. Neutron depolarisation study is an excellent tool to probe the magnetic inhomogeneity of samples. The neutron depolarisation study is a mesoscopic probe. It can measure spatial magnetic inhomogeneity on a length scale from  $100 \text{ \AA}$  to several microns. In an unsaturated ferromagnet or ferrimagnetic, the magnetic domains exert a dipolar field on the neutron

FIG. 5.1.9)

Mossbauer spectrum of  $\text{Fe}_{0.05} \text{Sb Se}_{0.025}$  sample

polarisation and depolarise the neutrons owing to Larmor precession of the neutron spins in the magnetic field of the domains

One would expect depolarisation for the case of clusters of spins (atleast of mesoscopic length scale) with net moments. The advantages of neutron depolarisation technique are the domain size information can be obtained (as an average over the entire sample), and there are essentially no resolution restrictions on the size of the domains, which can be measured.

The temperature in the present study was varied from 15K to 300K. The sample was cooled in zero field and then a 7 Oe external field was applied to study the depolarisation effect on the neutrons by the samples. The powder sample was used in the form of a pellet of cylindrical dimension. The sample was kept in the neutron beam in such a way that its plane surface remains perpendicular to the propagation direction of the polarised neutron beam. Also the beam size was restricted with cadmium slit, which is within the size of the samples. This experiment was carried out using the neutron polarisation analysis spectrometer (PAS) at Dhruva reactor, Trombay.

This study was carried out on the two samples of  $\text{Fe}_x\text{Sb}_{1-x-y}\text{Se}_y$  for  $X=0.002$ ,  $Y = 0.048$  and  $X=0.008, Y = 1.6$ . The temperature dependence of the transmitted neutron beam polarisation  $P$  with a field of 7 Oe. is depicted in the fig. 5.1E. This

value of P for all the samples over the entire range (15 to 297k) is found to be the same as the incident neutron beam polarisation ( $=986\pm 0.003$ ).

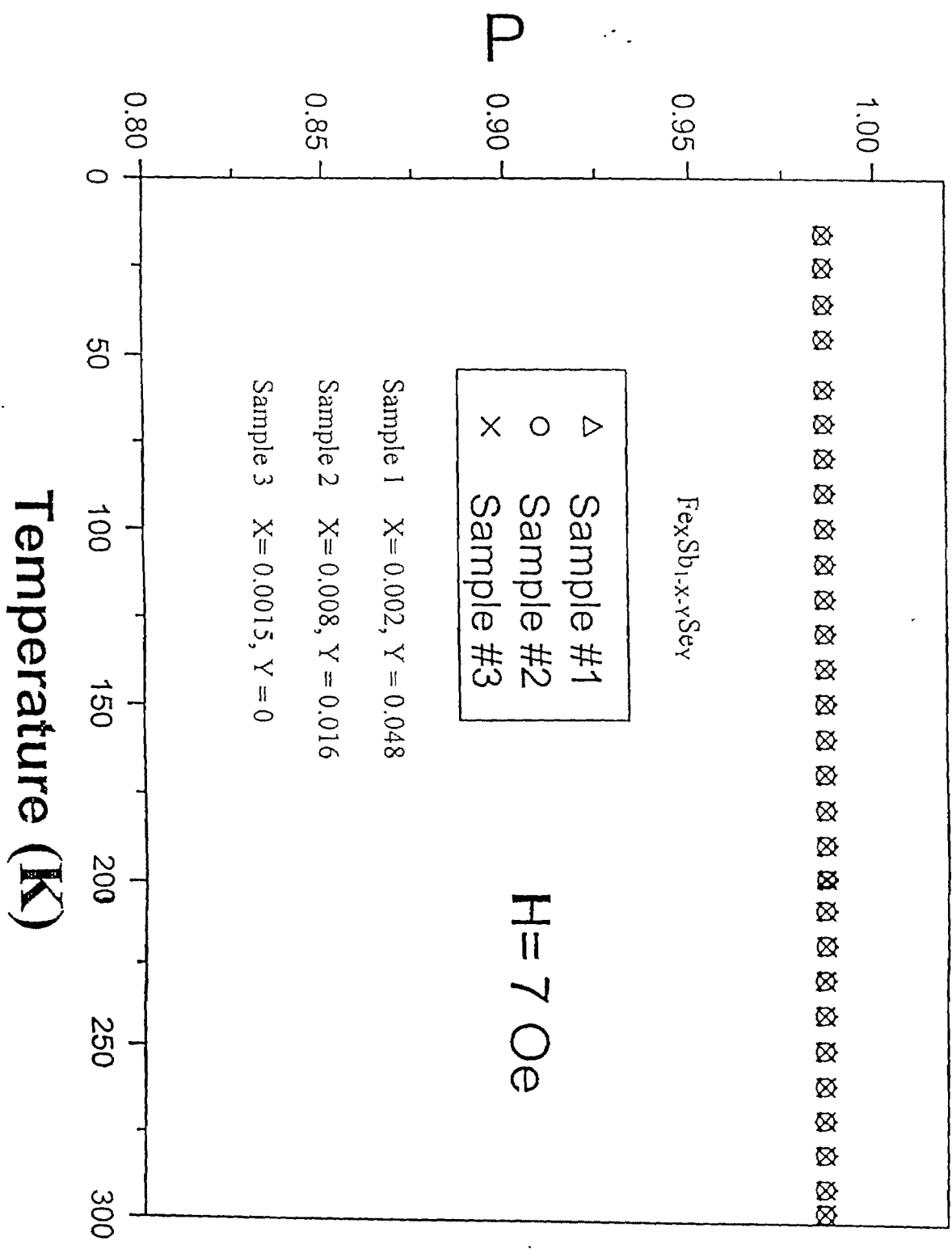
The study showed that there is no depolarisation for all the two Se samples over the entire range of temperature. Hence the absence of clusters of spins of Fe or Fe based compounds having net moments with a size about  $>100 \text{ \AA}$  was confirmed by this neutron depolarisation study Fig. 5.1E. If at all there are clusters it could be less than  $100 \text{ \AA}$  dimension. Thus formation of clusters of few atoms (nanoclusters) of Fe whose size is  $<100 \text{ \AA}$  may be producing the observed fields.

A second possibility is that if Fe atoms are dispersing uniformly at this concentrations one would expect an average distance of  $100 \text{ \AA}$  between two Fe atoms. Hence direct Fe interaction may not be possible.

In such case Fe can behave like an isolate ion surrounded by Sb ions and some Se ions. If the Fe do not interact in the neighbouring Sb/Se ions than one expect a local moment formation as was described in the case of low concentration FeSb systems in chapter 4.

The third possibility is the formation of magnetic Fe-Se compounds. Since the introduction of Se is bringing the magnetic field it is possible that Se is forming a magnetic compound with Fe. Fe and Se forms FeSe compound whose

Fig. 5.1 E



QS = 0.28(2) mm/sec (8). The second compound is that of FeSe<sub>2</sub>. The Mossbauer study of FeSe<sub>2</sub> compound showed QS of 0.584 (20) mm/sec (9). Both the compounds don't show magnetic interaction. The third compound phase is that of Fe<sub>7</sub>Se<sub>8</sub> which is known to be magnetic with a Curie temperature of 187°C (10). Temperature variation studies of some of these samples indicate that the Curie temperature of the samples are ~ 300 °C. Hence this type of compound formation can be also be ruled out (11).

Hence it can be argued that the magnetic interaction seen can be due to two type of interactions. The site A field value corresponding to ~310 KOe in case of X=0.002 and Y=0.004 sample may be due to isolated Fe ion not interacting with the neighbouring ions giving rise to the local moment. When Se is added to the system due to their large difference in their electronegativity (Fe 1.8 and Se 2.4 ) Se may be attracted towards Fe and if there is a partially antiferromagnetic coupling between Fe and Se it may result in the reduction of the field.

The second i.e. the site B field may be due to the RKKY interaction of Fe –Fe via Sb and Se. Introduction of Se may be bringing the conduction electron densities into the system and hence this type of interaction (RKKY) may be taking place. As more Se is introduced in the matrix it results in more Se going to the vicinity of Fe may result in a decrease in the field due to either screening effects or partial anti-ferromagnetic coupling as above or both.

**References :**

1. Diluted Magnetic Semiconductors, M. Jain (Eds.), World Sci., Singapore, 1991.
2. Semi Magnetic Semiconductors and Diluted Magnetic Semiconductors, M. Averous, M. Balkanski (Eds.), Plenum press, London, 1991.
3. J. Kossut, W. Dobrowolski, Handbook of Magnetic Materials, Vol. 7, K.H. J.Buschkow (Ed.), Elsevier Sci. Publ., B.V. Amsterdam, 1993, Chapter 4, 231-305.
4. Diluted Magnetic Semiconductors, vol. 25 of Semiconductors and semimetals, J.K. Furdyna, J. Kossut (Eds.), (R.K. Willardsson, A.C. Beer, Ser. Eds.), Academic press, Boston, 1988.
5. C. Benoit-La Guillaume, Handboo on semiconductors, T.S. Moss, S. Mahajan (Eds.), Elsevier Sci., B.V. Amsterdam, 1994, 507.
6. J.K. Furdyana, N. Samarth, J. Appl. Phys., 1987, 61, 3526.
7. W.J.M. De Jonge, H.J.M. Swagten, J. Magn. Magn. Mater., 1991, 100, 322.
8. B.K. Jain, A.K. Singh and K. Chandra, J. Phys. F., 8, 1978, 2625.
9. A.A. Temperley and H.W. Lefevre, J. Phys. Chem. Solids, 27, 1966, 85.
10. A. Okazaki, J. Phys. Soc. Japan, 16, 1961, 1162.
11. D.R.S. Somayajulu, Private Communication.

## **Chapter 6**

# **Multiple substitutions**

**in**

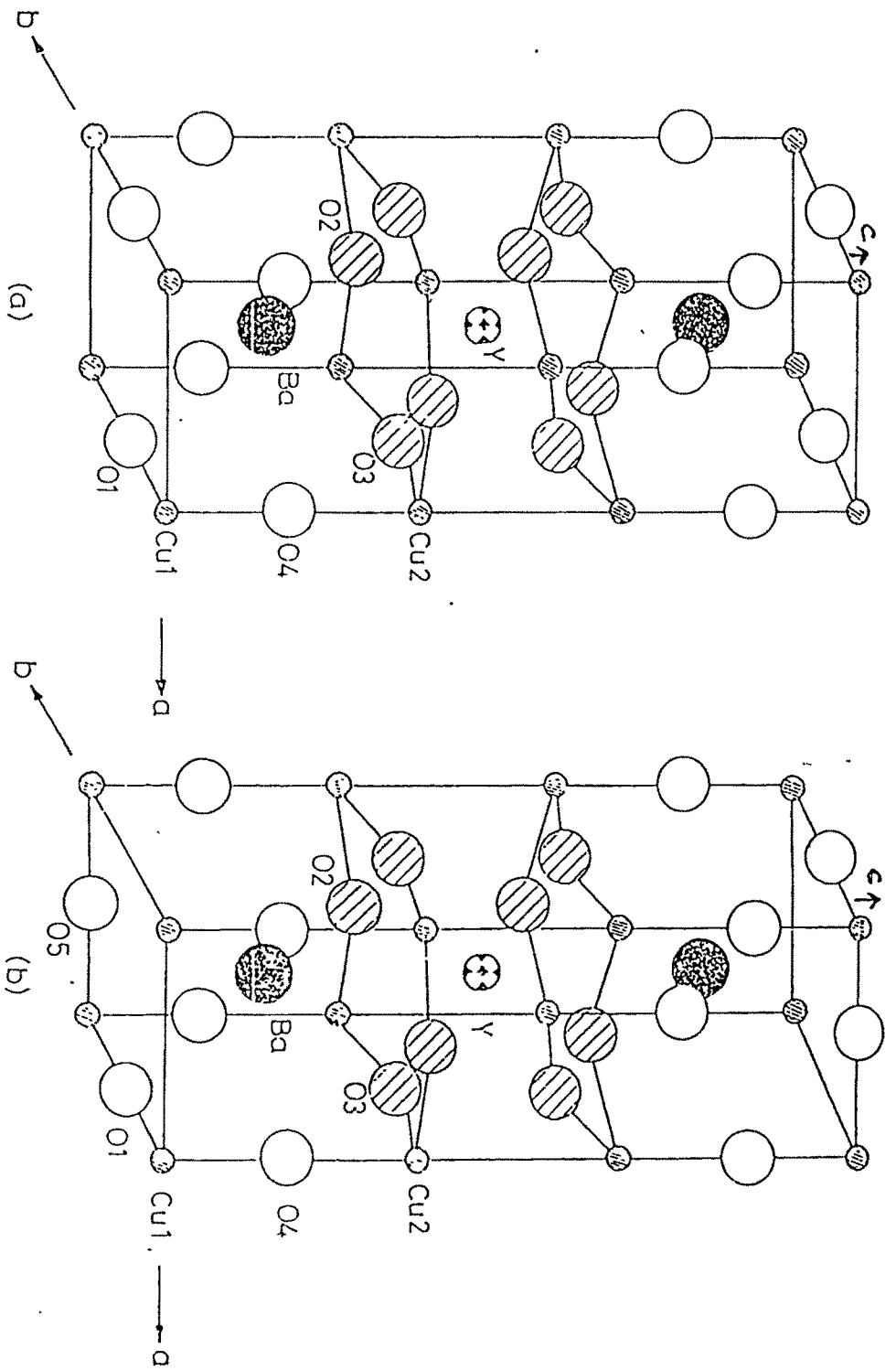
**YBCO**

## 6.1 Introduction:

The discovery of high  $T_C$  superconductors created tremendous interest and challenges to the existing understanding of the mechanism of superconductors (1,4). The transition temperatures of most of these superconducting compounds are well over 100K. Superconductivity above liquid nitrogen was discovered by Wu et. al. (4) in a multiphase compound in Y-Ba-Cu-O system. Soon it was established that it has a composition  $YBa_2Cu_3O_7$  (5).

$YBa_2Cu_3O_{7-\delta}$  (Y-123 or YBCO) has a orthorhombic distorted perovskite structure for  $\delta = 0$ , with unit cell consisting of two structurally inequivalent Cu sites: the Cu(I) or the chain site and Cu(II) or the plane site. As shown in the fig. [6.1 A (a and b)] the O(5) sites along the a-axis are vacant forming square planar Cu chains along b-axis (6) and with cell parameters  $a=3.82 \text{ \AA}$ ,  $b = 3.88 \text{ \AA}$  and  $c = 11.69 \text{ \AA}$ . This compound has a unique structure in which the Y and two Ba atoms occupy 8 fold and 10 fold oxygen coordination respectively. The lower  $T_C$  (60 K) phase is characterized by disordered O(5) vacancies resulting in transition from orthorhombic to tetragonal structure.

YBCO with  $\delta=1$  is tetragonal and has a cell parameter  $a=3.86 \text{ \AA}$  and  $c=11.84 \text{ \AA}$ . The disposition of the  $CuO_2$  plane and CuO chains is such that there is



Structure of  $\text{YBa}_2\text{Cu}_3\text{O}_7$ : (a) Orthorhombic (b) Tetragonal. As can be seen, in the latter, the  $\text{O}_1$  and  $\text{O}_5$  positions are randomly occupied.

Fig. 6.1 A

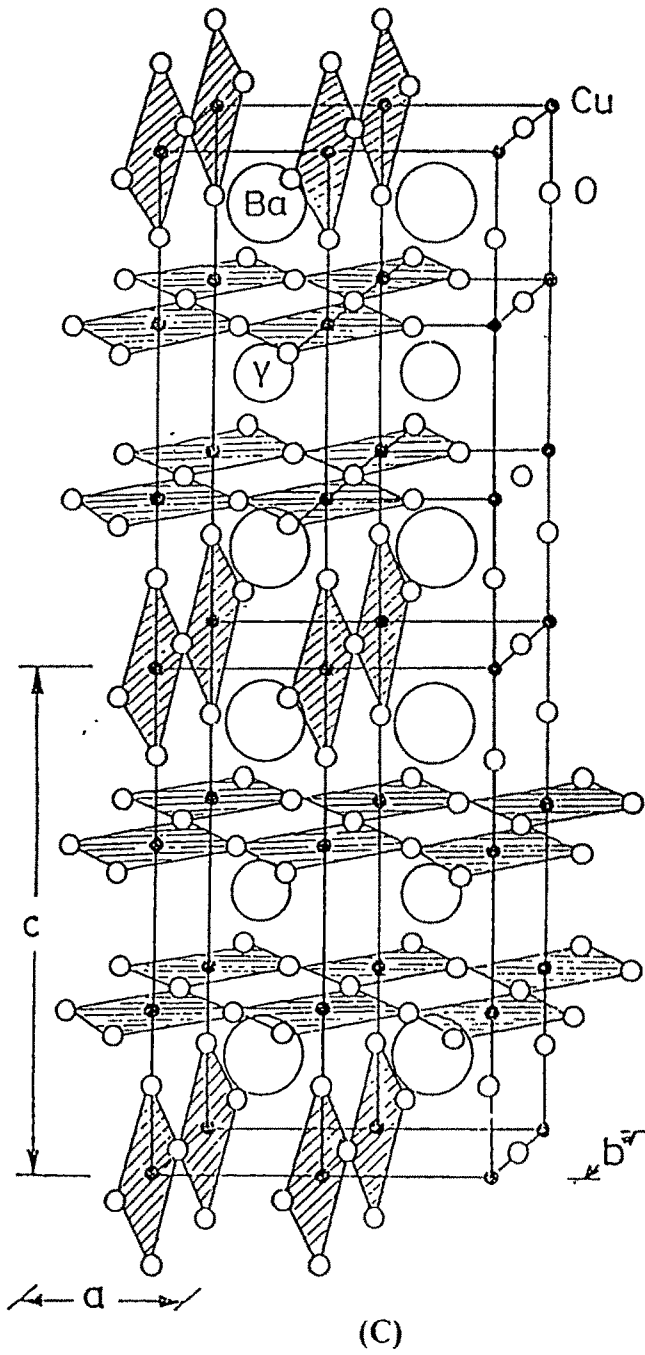


Fig. 6.1A

Structure of  $\text{YBa}_2\text{Cu}_3\text{O}_7$  showing the  $\text{CuO}_2$ - square planes and  $\text{CuO}$  linear chains.

significant interaction between the planes and chains. The fig. [6.1 A (C)] show the structure of YBCO's  $\text{CuO}_2$  square plain and the  $\text{CuO}$  linear chains. Here due to oxygen deficiency there exist mixed valence in Cu. The metallic conduction and the superconductivity are attributed to the planes with in the  $\text{YBa}_2\text{Cu}_3\text{O}_7$  structure with the chains enhancing the  $T_C$ . Substitutions in these high  $T_c$  superconductors were of great importance to find out the exact mechanism of superconducting behaviour. A great deal of studies has taken place in which partial mono substitutions were done at different sites in these superconductors.

A very interesting aspect of Y-123 compound is that when Y is replaced by other magnetic rare earths, the superconducting properties are not destroyed indicating that there is negligible interaction between the localised f-electrons of the rare earth ions and the conduction electrons of the Cu, which are responsible for the Cooper pair formation and superconductivity (7-12). All the  $\text{LnBa}_2\text{Cu}_3\text{O}_7$  (Ln rare earths) form isostructural compounds similar to  $\text{YBa}_2\text{Cu}_3\text{O}_7$ . However Ce, Tb and Lu do not form the 123 phase due to factors like size difference and greater stable phase of  $\text{BaCeO}_3$  and  $\text{BaTbO}_3$ . It is also well known that  $\text{Ca}^{2+}$  substitution at the  $\text{Y}^{3+}$  reduces the superconducting transition temperature of Y-123 for  $\delta=0$ .

But for  $\delta = 1$  sample, which is non conducting, 20 at. %  $\text{Ca}^{2+}$  at the  $\text{Y}^{3+}$  site makes the sample superconducting (13-16). The decrease in  $T_C$  was attributed to

overdoping of holes (17-19) while others suggested it due to the creation of vacancies and/or the oxygen disorder in the  $\text{CuO}_2$  plane (15,16). The observed effect is more pronounced in the oxygen deficient samples. Hence better understanding of oxygen disorder or vacancies in-and-round  $\text{CuO}_2$  plane in Y-123 compound is essential as superconducting charge carriers are supposed to reside in this plane.

Substitutions at the Ba site include the Lanthanides and other alkaline earth elements. In  $\text{Y}(\text{Ba}_{2-x}\text{Sr}_x)\text{Cu}_3\text{O}_7$ , the solid solubility exist only upto  $X=1.0$  and  $T_c$  decreases with increase of  $X$ . (20-25). Also some reports exists on the substitution of Mg and K at the Ba site but it is not definitely known whether these ions enters the lattice (24-25). During the substitution studies at the Y and Ba sites a new phase was seen having the formula  $\text{CaLaBaCu}_3\text{O}_7$  where  $\text{Y}^{3+}$  is replaced by  $\text{Ca}^{2+}$  and  $\text{Ba}^{2+}$  replaced by  $\text{La}^{3+}$  having a tetragonal structure and showed superconductivity in the range of 75-80K.

Metal dopants substituted at the Cu site systematically alter the superconducting temperature and the crystal structure. (26,27). Studies on the effect of Ti, V, Cr, Mn, Fe, Co, Ni, Nb, Mo, Pt, Zn, Cd, Ga, and Ag doping were carried out by substituting these ions at the Cu site. Depending on the ionic size and the electronic configuration only certain elements can replace Cu in Y-123 compound. For example Ag doesnot enter the lattice at all. From these studies it

was inferred that it is the CuO plane and not the CuO chain which is responsible for the superconducting behaviour (28).

Dopants like Mg, Zn, Ni which are divalent preferentially occupy the Cu-O plane replacing the  $\text{Cu}^{2+}$  ions and hence causes a sharp decrease in the  $T_c$ . Dopants like Fe, Co, Al and Ga which cause some what less drastic depression in the  $T_c$  are found to replace linear Cu chain site at low concentrations(29). Also it has been found that oxygen content also plays a crucial role in the site occupancy of these dopants

The 3d ion doping at the Y-123 has been studied extensively but relatively few studies are done on the Ca based  $\text{CaLaBaCu}_3\text{O}_7$  (1113) compound. This system has a tetragonal crystal structure (30-33) with  $T_c$  around 75 K. The lattice parameter is  $a = 3.869\text{\AA}$  and  $c = 11.645\text{\AA}$ . Yamaya et. al (33) have studied the oxygen deficient samples of LBCCO and they found that the system remains tetragonal for all values of the oxygen content investigated by them. The resistivity of the oxygen deficient samples is found to be similar to that of the oxygen deficient YBCO systems. (34). It is also found that the  $T_c$  of the Fe doped system decreases drastically compared to Y-123 systems. The local magnetic moment decreases with increase in the Fe concentration. The c-parameters is found to be compressed with the Fe concentration (35).

The present study aims at finding the effect of multiple substitutions in Y-123 to find out the effect of various substitutions on charge balancing, oxygen content and site occupancy. Also effect of Fe doping in LBCCO, its relation to the site occupancy, charge state of Fe and characterisation at the microscopic level are also studied using Mossbauer spectroscopy. A comparative study is done with doped Y-123 compounds too.

## 6.2 Experimental:

Samples with general formula  $(Y_{1-z}Ca_z)Ba_2(Cu_{1-x-y}Fe_yM_x)_3O_{7-δ}$  were prepared through solid state reaction route. Stoichiometric quantities of (99.99%) pure dry  $Y_2O_3$ ,  $CaCO_3$ ,  $BaCO_3$ ,  $Fe_2O_3$ ,  $CuO$  and oxides of Co, Ni, Zn, Cr, carbonates of Mn were taken and mixed thoroughly and calcinated at 930 °C in air for 24 hours. The calcinated powder was ground, mixed pelletised and annealed at 930 °C in air for 24 hours and slowly cooled (>72hr) to 200 °C.

The whole annealing process was repeated twice. All the samples were annealed simultaneously in a box furnace having temperature variation of  $\pm 10$  °C between its corners. All the samples were also treated in flowing oxygen too. Phase identification was carried out by XRD. The lattice oxygen content was estimated through iodometric titration (36). Mossbauer spectra of the samples

were recorded at room temperature with  $\text{Co}^{57}$  in Rh matrix as the source. The spectra were least square fitted with a computer program.

The samples with the composition  $\text{LaBaCaCu}_{3-x}\text{Fe}_x\text{O}_7$  (where  $x = 0.03, 0.18 \text{ \& } 0.24$ ) were prepared by thoroughly mixing and grinding of  $\text{La}_2\text{O}_3$ ,  $\text{BaCO}_3$ ,  $\text{CaCO}_3$ ,  $\text{CuO}$  and  $\text{Fe}_2\text{O}_3$  in stoichiometric ratio and firing at  $975^\circ\text{C}$  for 12 hours. The samples were cooled to room temperature by air quenching. The exercise was repeated three times. The powders were grounded and heated at  $975^\circ\text{C}$  in air for 12 hours before furnace cooling to room temperature. The pressed pellets were annealed at  $575^\circ\text{C}$  in flowing oxygen for 24 hours and were furnace cooled to room temperature over a span of 110 hours. XRD was done to find the phase of the samples (35).

### 6.3 Results and Discussion:

The figures 6.1B and 6.1C shows typical XRD patterns recorded using  $\text{CuK}_\alpha$  obtained for some of the compositions with the formula

Table 6.1 A

General formula:  $(Y_{1-Z}Ca_Z)Ba_2(Cu_{1-X-Y}Fe_YM_X)_3O_{7.8}$

Composition of the samples				Lattice parameters		Oxygen Content
	X	Y	Z	A Å	B Å	Without Oxygenation
	.00	.08	.00	3.861	11.672	6.47
	.00	.14	.00	3.876	11.686	6.62
						With extensive oxygenation
	.00	.08	.10	3.854	11.710	6.59
	.00	.08	.20	3.869	11.746	6.53
<b>Ni</b>	.02	.08	.20	3.867	11.679	6.47
	.04	.08	.20	3.842	11.686	6.53
<b>Zn</b>	.02	.08	.20	3.844	11.614	6.61
	.04	.08	.20	3.865	11.562	6.54
<b>Co</b>	.02	.08	.20	3.859	11.626	6.68
	.04	.08	.20	3.855	11.625	6.62
<b>Mn</b>	.02	.08	.20	3.853	11.652	6.76
	.04	.08	.20	3.845	11.603	6.80
<b>Cr</b>	.02	.08	.20	3.861	11.635	6.68
	.04	.08	.20	3.865	11.655	6.70

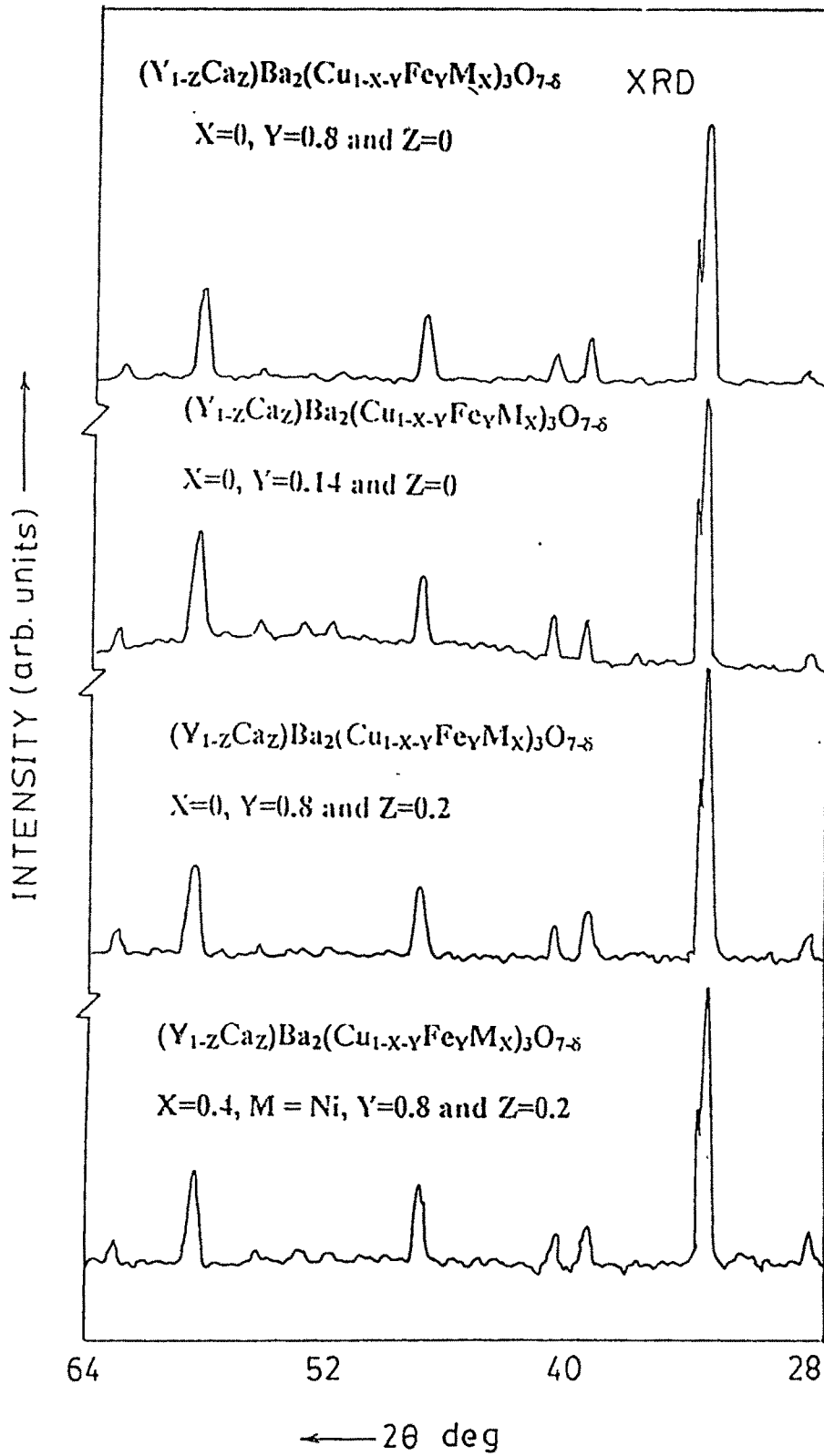


Fig. 6.1 B

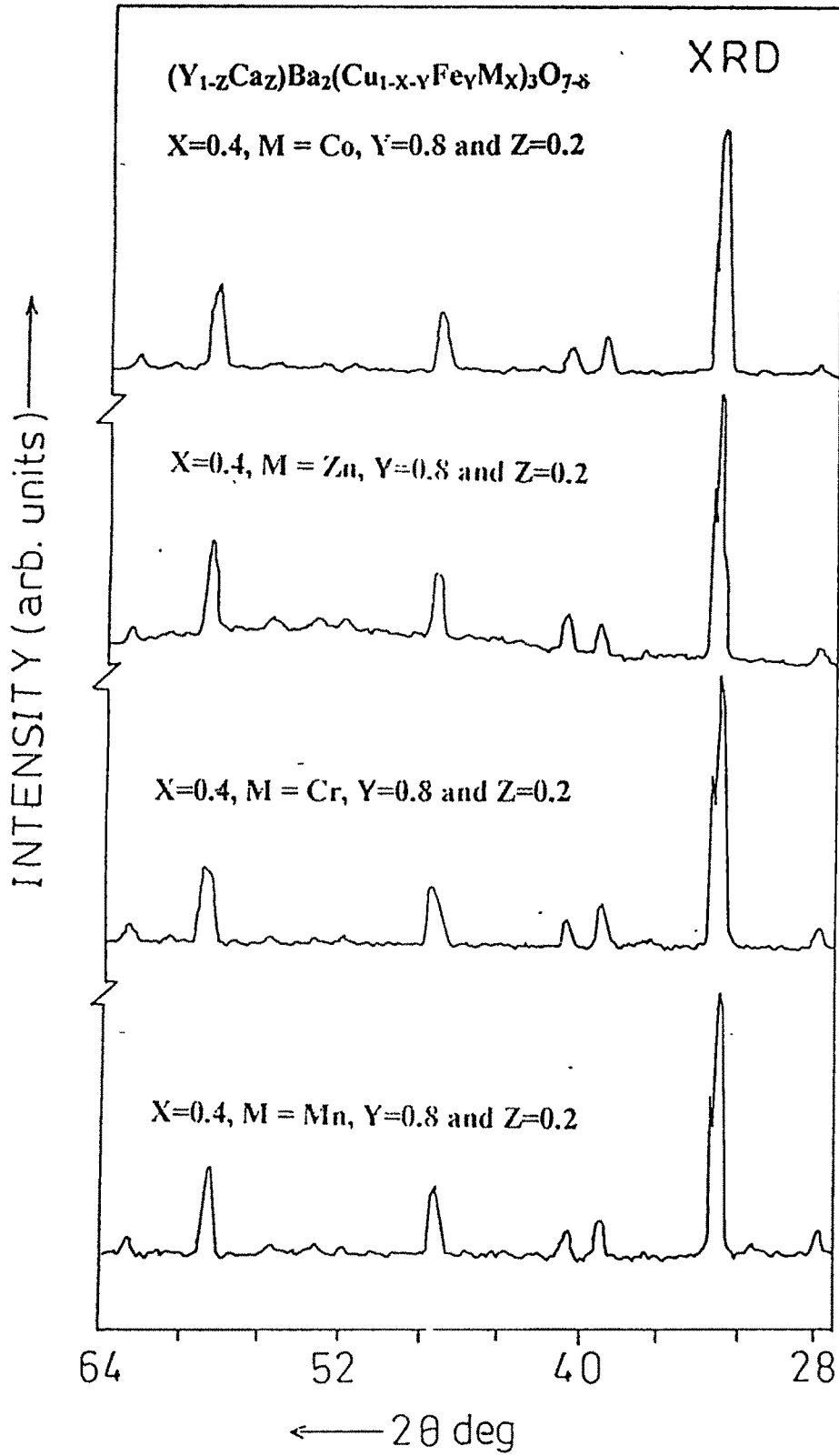


Fig. 6.1 C

$(Y_{1-z}Ca_z)Ba_2(Cu_{1-x-y}Fe_yM_x)_3O_{7-\delta}$ . Crystallographic lattice parameters calculated through Rietveld refinement for the single 123 phase composition are listed in the Table 6.1A. It is evident that all the samples exhibit single tetragonal phase formation. Lattice oxygen content determined through iodometric titration for the samples are also listed in the table 6.1 A. All the  $Ca^{2+}$  substituted samples were prepared with 20 at. % of Ca which is the optimum limit for the formation of single tetragonal phase of Y-123.

Local environment of Fe was investigated through Mossbauer technique. The Mossbauer spectra were recorded at room temperature with  $Co^{57}$  in Rh matrix as the source. The results of the Fe Mossbauer study carried out to determine the coordination and relative site population of Fe in each of these samples are shown in Table 6.1B. The Mossbauer spectra of the multiple substituted YBCO are given from Fig. 6.1.1 to 6.1.14. The area under the curve tells us about the site occupancy of the Fe ions. The value of the Quadrupole splitting (QS) tells about type of coordination.

It is well known that well oxygenated Fe doped YBCO samples has  $\delta \sim 7.0$ . But in the present case when 10%  $Ca^{2+}$  was substituted at the  $Y^{3+}$  site the oxygen content decreased to  $\sim 6.59$ . When the  $Ca^{2+}$  substitution was increased to 20% of  $Y^{3+}$  the value of oxygen content decreased still further. Similarly from the table 6.1A it can be seen that the samples containing Ca have rather low oxygen content

**Table No. 6.1 B**  
**General formula :  $Y_{1-z}Ca_zBa_2(Cu_{1-x-y}Fe_yM_x)_3O_{7.5}$**

Composition of samples				Quadrupole Splitting (mm/sec)			Isomer Shift (mm/sec)			Area under the curve (%)		
	X	Y	Z	Cu(I)		Cu(II)	Cu(I)		Cu(II)	Cu(I)		Cu(II)
				A	B	C	A	B	C	A	B	C
	.00	.08	.00	2.00	1.25	0.39	-0.10	-0.08	-0.14	.189	.394	.417
	.00	.14	.00	2.03	1.27	0.57	-0.03	-0.06	-0.06	.407	.274	.319
	.00	.08	.10	1.93	1.20	0.41	-0.04	-0.05	-0.15	.427	.292	.281
	.00	.08	.20	2.07	1.90	0.66	-0.07	-0.01	-0.16	.304	.266	.430
Ni	.02	.08	.20	2.00	1.11	0.38	-0.08	-0.29	-0.29	.494	.198	.308
	.04	.08	.20	1.97	0.93	0.42	-0.06	-0.16	-0.26	.625	.172	.203
Zn	.02	.08	.20	1.99	0.96	0.47	-0.04	-0.21	-0.16	.580	.247	.173
	.04	.08	.20	1.99	0.80	0.33	-0.07	-0.26	-0.19	.516	.333	.150
Co	.02	.08	.20	2.04	1.29	0.43	-0.09	-0.10	-0.16	.549	.160	.291
	.04	.08	.20	2.03	1.15	0.42	-0.09	-0.15	-0.16	.399	.254	.352
Cr	.02	.08	.20	2.05	1.08	0.43	-0.12	-0.10	-0.18	.496	.247	.257
	.04	.08	.20	2.01	1.28	0.34	-0.10	-0.14	-0.16	.291	.414	.295
M	.02	.08	.20	2.06	1.54	0.47	-0.09	-0.05	-0.22	.312	.398	.290
n	.04	.08	.20	2.02	1.04	0.36	-0.02	-0.04	-0.19	.452	.192	.356

The experimental error for the site occupancy is .007

The experimental error for the value of QS is .01.

The experimental error for the value of IS is .01

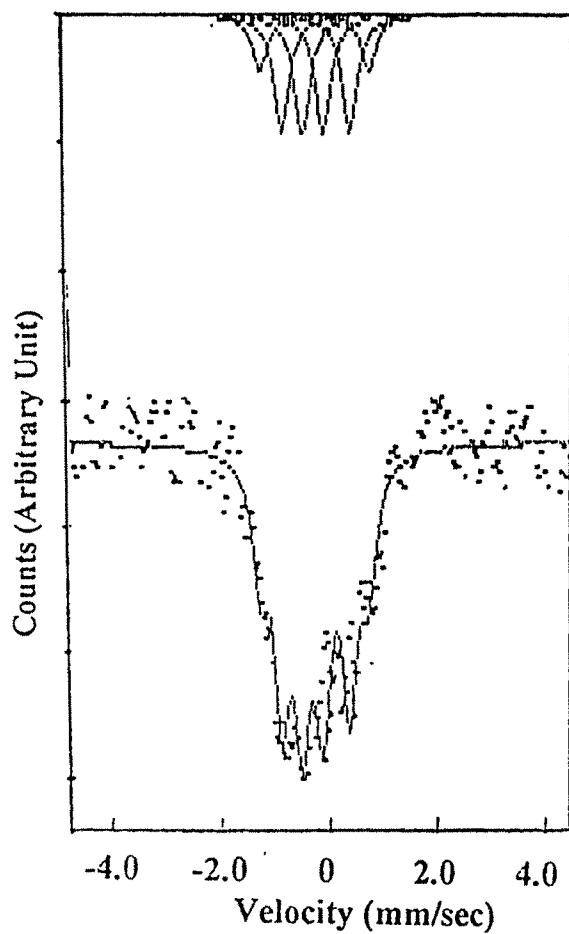


Fig. 6.1.1

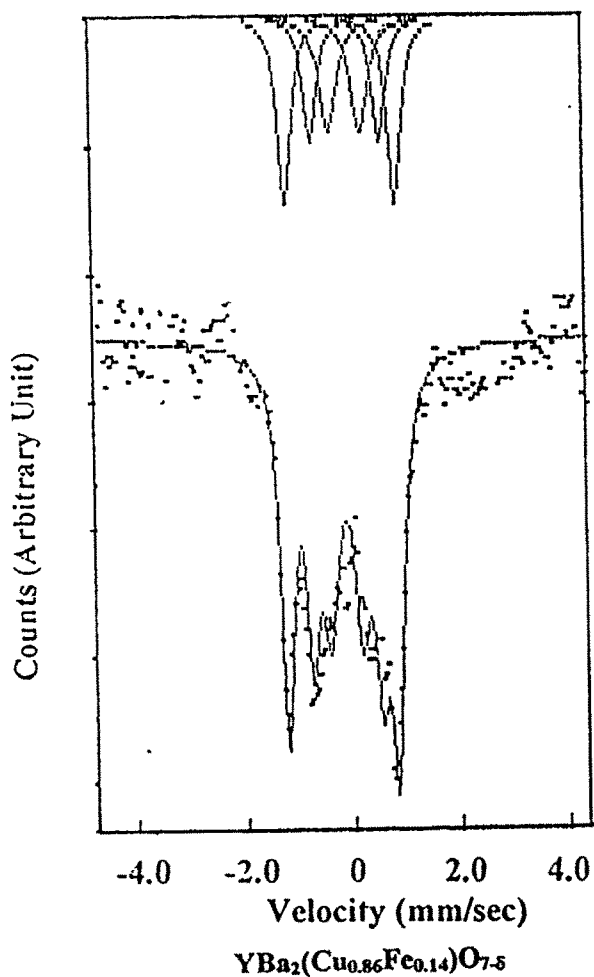
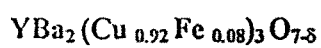


Fig. 6.1.2



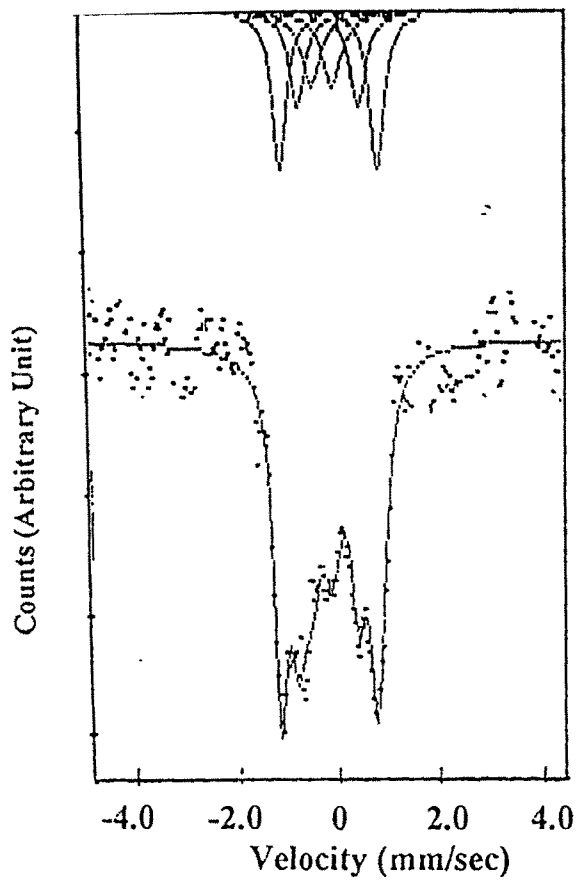


Fig. 6.1.3

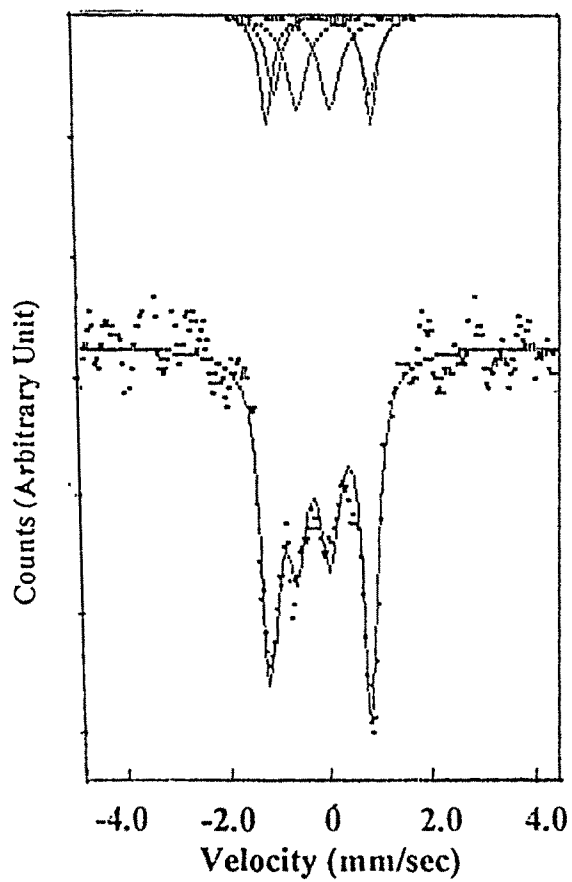
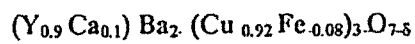
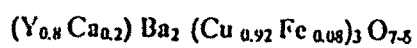


Fig. 6.1.4



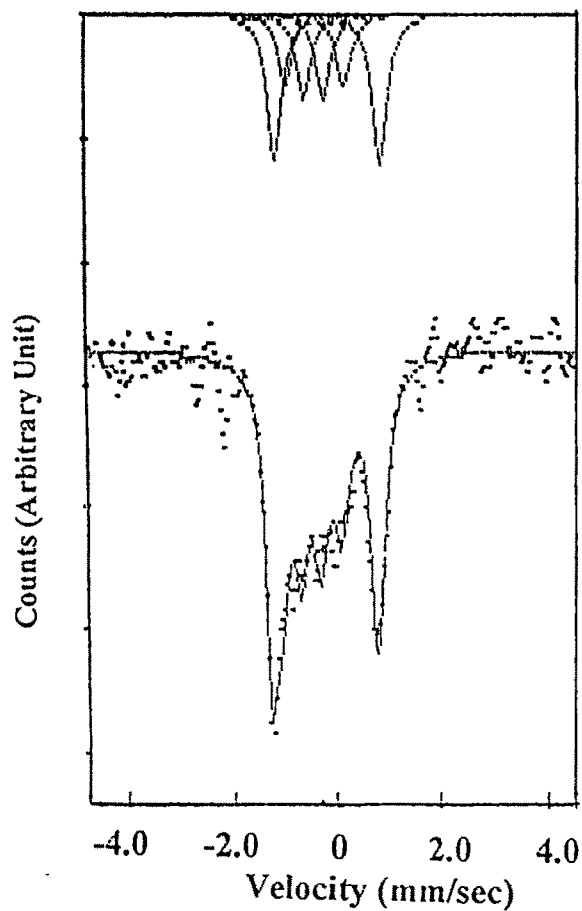


Fig. 6.1.5

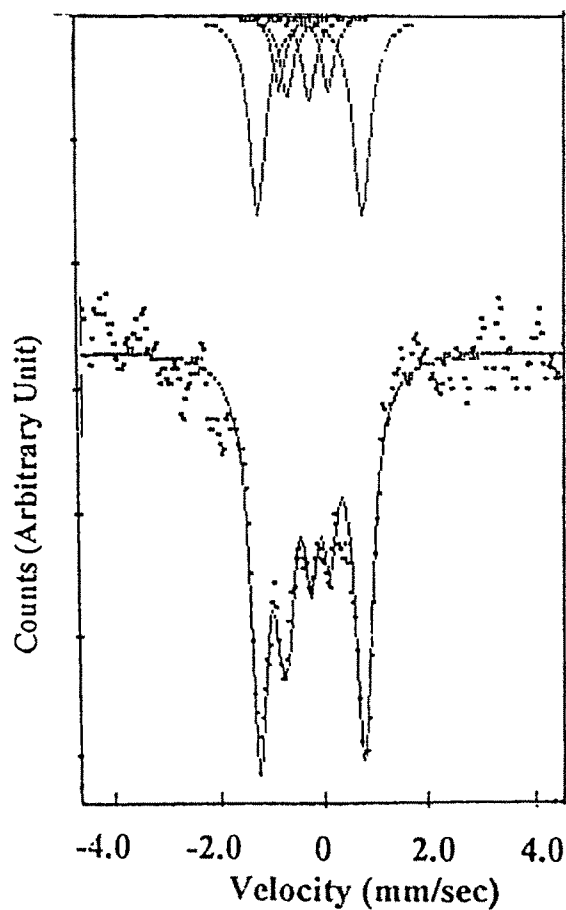
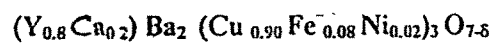
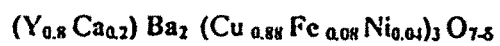


Fig. 6.1.6



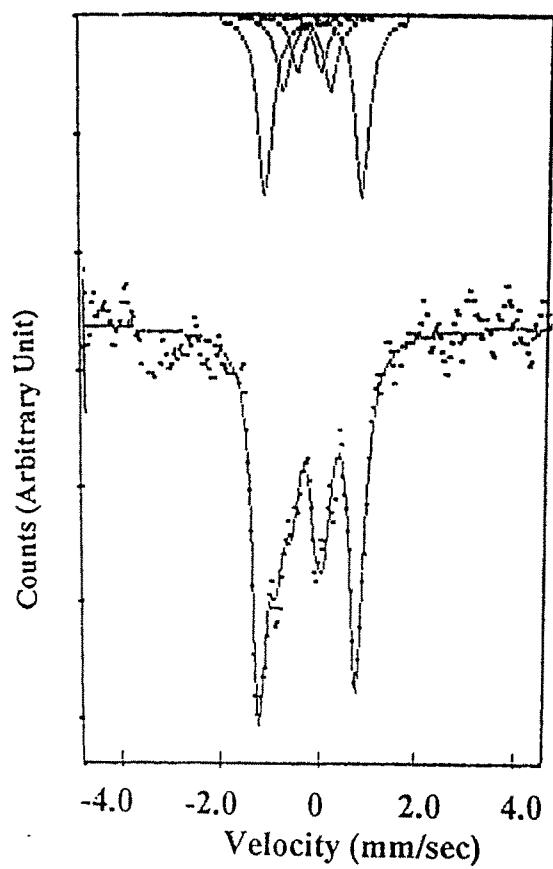


Fig. 6.1.7

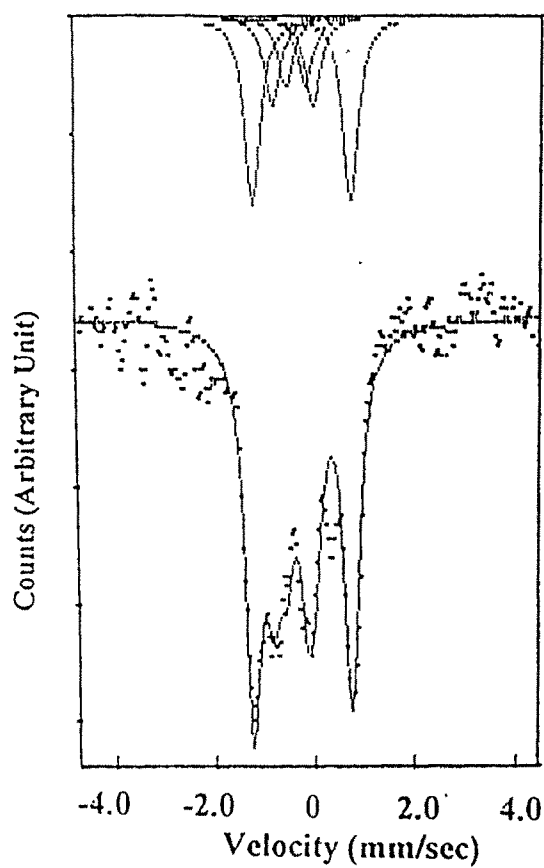
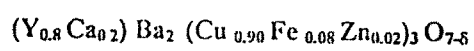
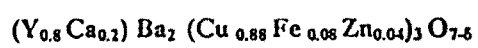


Fig. 6.1.8



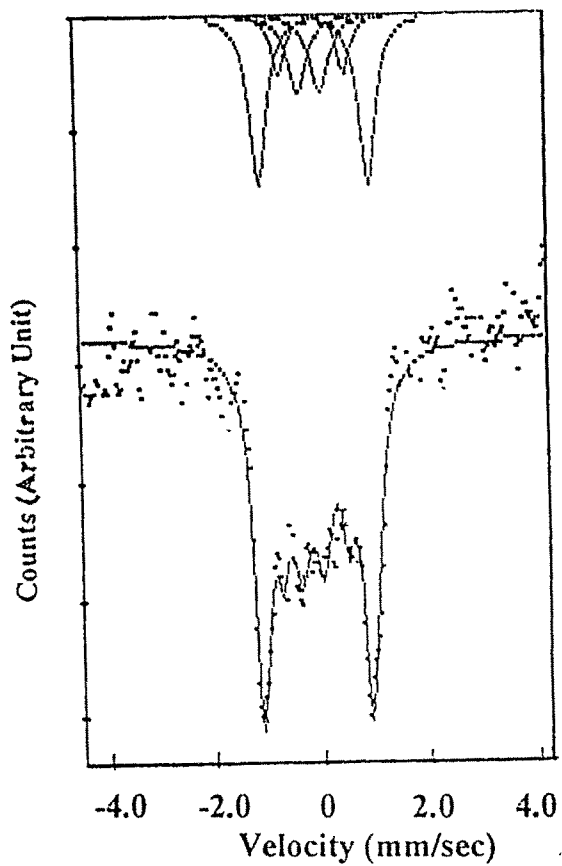


Fig. 6.1.9

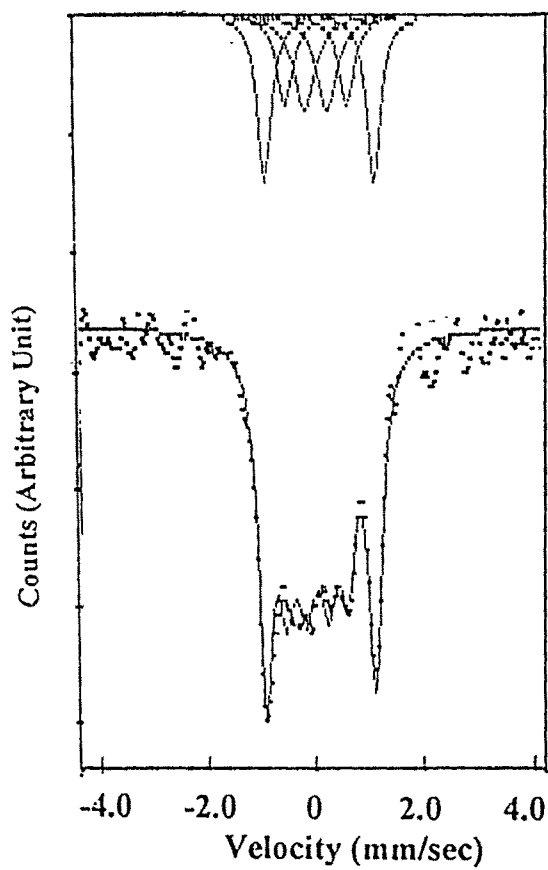
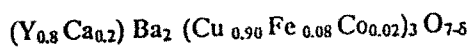
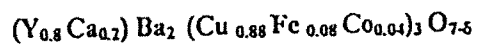


Fig. 6.1.10



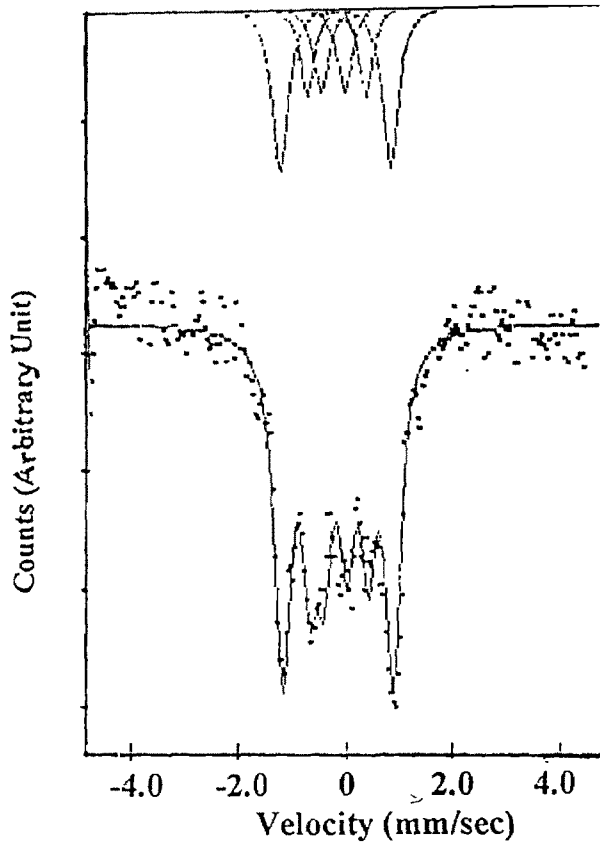


Fig. 6.1.11

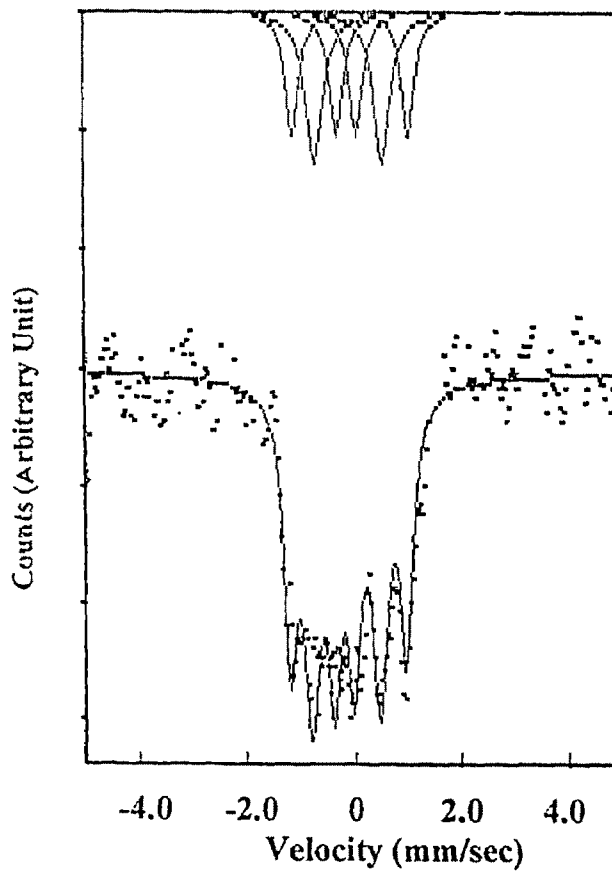
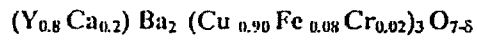
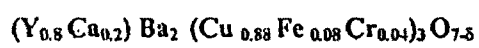


Fig. 6.1.12



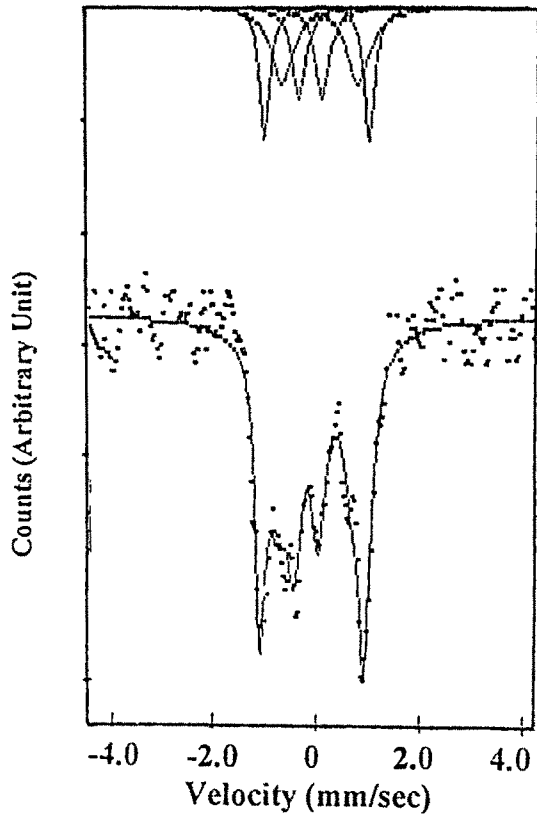


Fig. 6.1.13

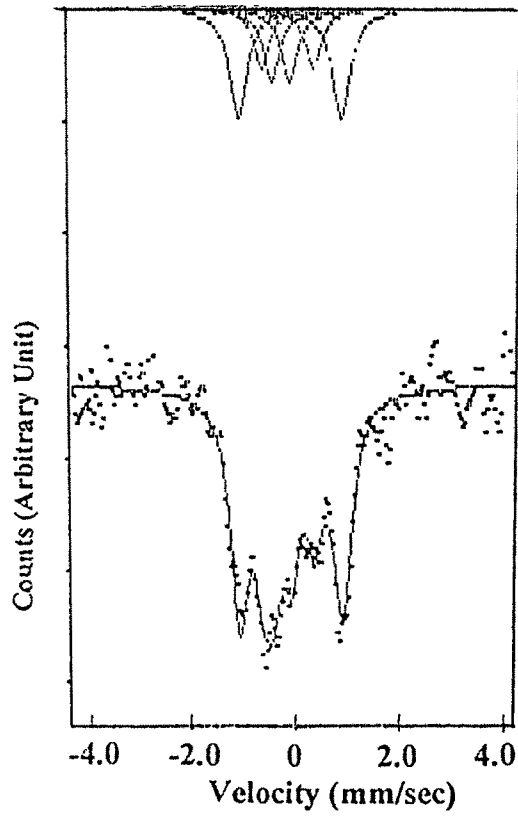
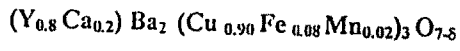
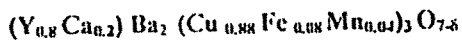


Fig. 6.1.14



even though they were oxygenated extensively and annealed in flowing oxygen for >72 h. Even the presence of oxygen getter elements like Fe and Co at Cu site do not enhance the intake of oxygen. But the presence of Fe (14%) without  $\text{Ca}^{2+}$  substitution was able to enhance the intake of oxygen even when the sample was annealed in air and not in flowing oxygen. This suggests that no over doping of holes take place when  $\text{Ca}^{2+}$  is substituted at  $\text{Y}^{3+}$  site in 123 compound. Similar observations were reported by others (15-17).

Earlier we observed that the presence of  $\text{Ca}^{2+}$  at the  $\text{Y}^{3+}$  site with  $\text{Sr}^{2+}$  substituted at  $\text{Ba}^{2+}$  site showed substantial increase in lattice oxygen content even when annealed in air. This was attributed to the size effect that was produced when small  $\text{Sr}^{2+}$  ion was substituted in place of larger  $\text{Ba}^{2+}$  ion. The observed enhancement of oxygen content was attributed to relaxation of chemical pressure in the Ba/Sr-(04) layer close to the Cu(I) chain site (37). Also these compositions resulted in highest recovery of  $T_c$  value (38). Earlier study in this regard on  $\text{Y}(\text{Ba}_{2-y}\text{Sr}_y)\text{Cu}_3\text{O}_{7.8}$  showed reduction in the lattice oxygen content with  $y$  and introduction of vacancies in the Cu(I) chain site (39).

Analysis of the Fe Mossbauer results was carried out to determine the site occupancy and coordination number in the substituted samples. The best fitting was obtained when the samples were least square fitted with three doublets showing Fe to have three different environments. Information regarding the type

of coordination is extracted from the values of QS where as area under the curve tells us about the site occupancy and its relation with oxygen content that can be inferred.

The analysis of the data shows that Fe substituted at Cu(I) site has two different oxygen configurations, two /three fold distorted square planar (A) and a five fold pyrimidal oxygen coordination (B). The Fe going to Cu(II) site has only one type of coordination that is a distorted five-fold pyrimidal oxygen coordination (C).

For Fe 8% sample with an oxygen content of ~6.5 about 58% of Fe goes to Cu(I) site and remaining 42 % of Fe goes to Cu(II) site. This shows the affinity of Fe towards oxygen. More oxygen present in CuO<sub>2</sub> plane site induced substantial amount of Fe to go to this Cu (II) site even though Fe goes predominantly to Cu(I) chain site. When the Fe concentration was increased to 14% it was observed that the oxygen content increased although the samples were given similar heat treatment in air. This resulted in more Fe going to Cu(I) site compared to 8% Fe sample due to the availability of more lattice oxygen in Cu(I) chain site.

All the Ca<sup>2+</sup> substituted samples were given similar heat treatment. Hence it was expected that the values of percentage site occupancy of Fe to remain almost constant with in the experimental limits. But Mossbauer analysis of the

peak area and QS suggest that percentage of Fe in both sites Cu(I) and Cu(II) changes with the substitution of 3-d transition elements. It can be said that Ni and Zn shifts Fe from Cu(II) to Cu(I) site. This points to the fact that these substituted 3d ions are going to Cu(II) site. In case of Zn 4% sample the percentage occupancy of Fe in Cu(II) site is much lower (~15%) compared to  $\text{Ca}^{2+}$  sample substituted at  $\text{Y}^{3+}$  site with  $X=0$ , even though the oxygen content in these cases are the same. This indicates the importance of site occupancy of the 3d-ions and its relation to Fe site occupancy. Similarly Co and Cr seems to prefer Cu(I) site and are responsible to make Fe go to Cu(II) site.

There was some ambiguity in the result of Mn due to either statistics or overlapping of different signals. In case of Mn substitution, even though the oxygen content of these samples were the maximum, still ~ 29% of Fe goes to Cu(II) site for Mn 2% sample and ~36% of Fe goes to Cu (II) site for Mn 4% sample. Further the high oxygen content (~6.8) in the lattice decreased the percentage site occupancy (35%) when compared to the Ca 20% with  $X=0$  sample where a low oxygen content ~6.53 forced 43% of Fe to go to Cu(II) site. This indicate that it is the site occupancy of the 3d ion that forces Fe to switch between the Cu(I) and Cu(II) sites depending on the site occupancy of 3d-ions and also on the lattice oxygens. In the present case Mn forces Fe to go from Cu(I) to Cu(II) site which points to the fact that Mn prefers Cu(I) site.



The value of QS suggests that the two sites for Fe at Cu(I) site are: A square planar configuration (A) resulting in large QS and a more symmetric five fold pyramidal site (B). Cu(II) site has a unique five fold distorted pyramidal configuration which seem to be much more symmetric with respect to site B of Cu(I) plane. The Isomer shifts also indicate that Fe is predominantly in 3+ charge state in these substituted superconductors.

It can be concluded from the present result that the percentage site occupancy of Fe at the Cu(I) and Cu(II) sites depends only on the availability of lattice oxygen and the site occupied by the 3-d ion. The hole doping due to presence of  $\text{Ca}^{2+}$  at  $\text{Y}^{3+}$  site seems to have no direct relation on the percentage site occupancy of Fe at any particular Cu site. Also Ca hinders the intake of oxygen in to the 123 lattice.

Further though oxygen distortions are expected in  $\text{CuO}_2$  plane and in Cu-O chains due to multiple substitutions in YBCO, no oxygen vacancies in  $\text{CuO}_2$  plane is observed as Cu(II) site is found to retain distorted five fold pyramidal coordination only. This observation is in variance with some of the earlier studies (16, 40).

The present study also indicates that Cr, Co and Mn preferentially occupy Cu(I) site where as Ni and Zn prefers Cu(II) site.

#### **6.4 Concentration Dependence study of Fe doping in LaBaCaCu<sub>3-x</sub>Fe<sub>x</sub>O<sub>7</sub> system and its comparison with Y-123 systems :**

A study of concentration dependence of Fe in LaBaCaCuO<sub>3</sub>O<sub>7</sub> (1113) superconductor is done to see the effect on the structure, site occupancy and charge state of Fe. The interest in this compound is that it has a structure similar as tetragonal Re-123, with both the O(1) and O(5) sites completely occupied and hence no structural changes are observed in them even after substitutions of 3-d ions in place of Cu in this system (41,42).

In these samples the c-parameters get compressed due to the lower ionic size of Fe in comparison to Cu. Also the system retains tetragonal structure till the maximum limit of 8% of Fe studied in this case. It is also observed that in case of Zn doped 1113 the lattice parameters remain almost same. Also the oxygen content of these samples remain almost constant around 6.86. The value of T<sub>c</sub> in case of Fe doped as well as Zn doped 1113 decreases but there is a drastic effect in case of Fe doping than Zn doping (35,42).

One of the earlier studies indicated that for Fe doped 1113 system the value of T<sub>c</sub> decreases drastically compared to the Fe doped Re-123 systems. The local magnetic moment decreases with the increase in Fe concentration (42). The

present study of Fe doped 1113 was done for the first time using Mossbauer spectroscopy. In the present case the study was done at three concentrations 1%, 6% and 8% of Fe substituted at the Cu site and the Mossbauer spectra were recorded at room temperature. The lowest concentration sample was made using Fe-57 powder and the Mossbauer parameters are listed in Table 6.1C. The Mossbauer spectra of Fe doped La-1113 are shown in Fig. 6.1.15 to 6.1.17.

The spectra were least square fitted with two quadrupole doublets. The smaller Quadrupole splitting (QS) corresponds to Fe at Cu(I) site with a distorted six fold symmetry where as the larger splitting was attributed to the Fe in Cu(II) site having five fold pyramidal symmetry. In case of Re-123 QS of Fe at Cu(I) site varies between 1.3-2.0 mm/sec which points to the fact that Fe has distorted four and five fold coordination. But in the case of 1113 due to six fold coordination Fe shows a small and single QS of  $\sim 0.7$  mm/sec.

Also in case of Re-123 the QS at Cu(II) site is small ( $\sim 0.50$  mm/sec) but Fe doped 1113 system shows a large QS of ( $\sim 1.4$  mm/sec) showing a reduction in puckering in this plane. The value of Isomer Shifts for both the sites shows that Fe is predominantly in  $Fe^{3+}$  state. In Re-123 systems the Fe site occupancy depends on the availability of lattice oxygen content. At large value of oxygen content Fe predominantly go to Cu(I) site in case of Fe doped YBCO systems.

Table 6.1 C

Concentration Of Fe in $\text{LaBaCaCu}_{3-x}\text{Fe}_x\text{O}_7$	Quadrupole Splitting		Isomer Shift		Area under the curve(%)	
	1%	$0.75 \pm 0.03$	$1.43 \pm 0.03$	$-0.07 \pm 0.02$	$-0.05 \pm 0.02$	0.65
6%	$0.59 \pm 0.03$	$1.25 \pm 0.03$	$-0.17 \pm 0.02$	$-0.18 \pm 0.02$	0.53	0.47
8 %	$0.59 \pm 0.03$	$1.35 \pm 0.03$	$0.03 \pm 0.03$	$-0.09 \pm 0.02$	0.36	0.64

The experimental error for the site occupancy is .007

The experimental error for the value of QS is .01.

The experimental error for the value of IS is .01

Fig. 6.1.15

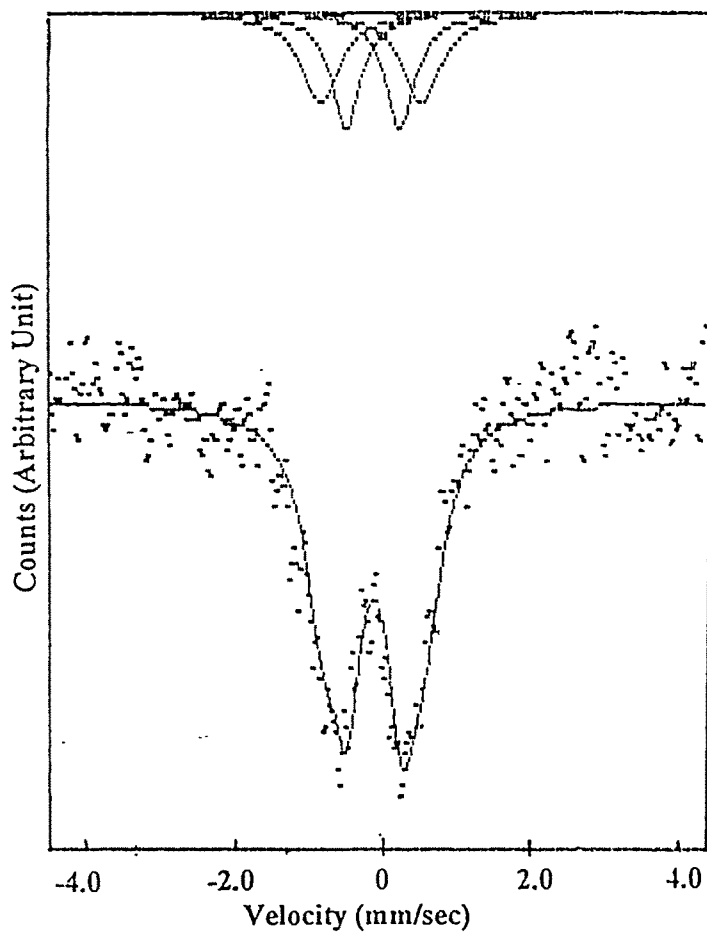
 $\text{LaBaCaCu}_3\text{Fe}_x\text{O}_{7.8}$ ;  $x = .03$ 

Fig. 6.1.16

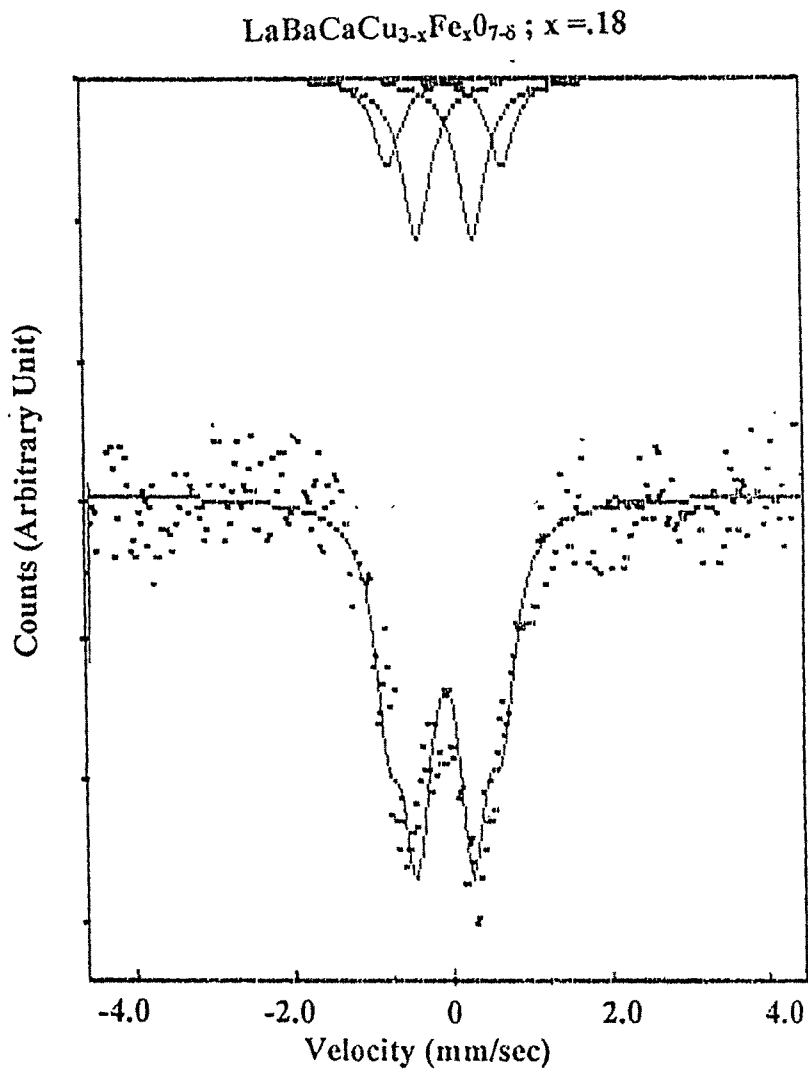
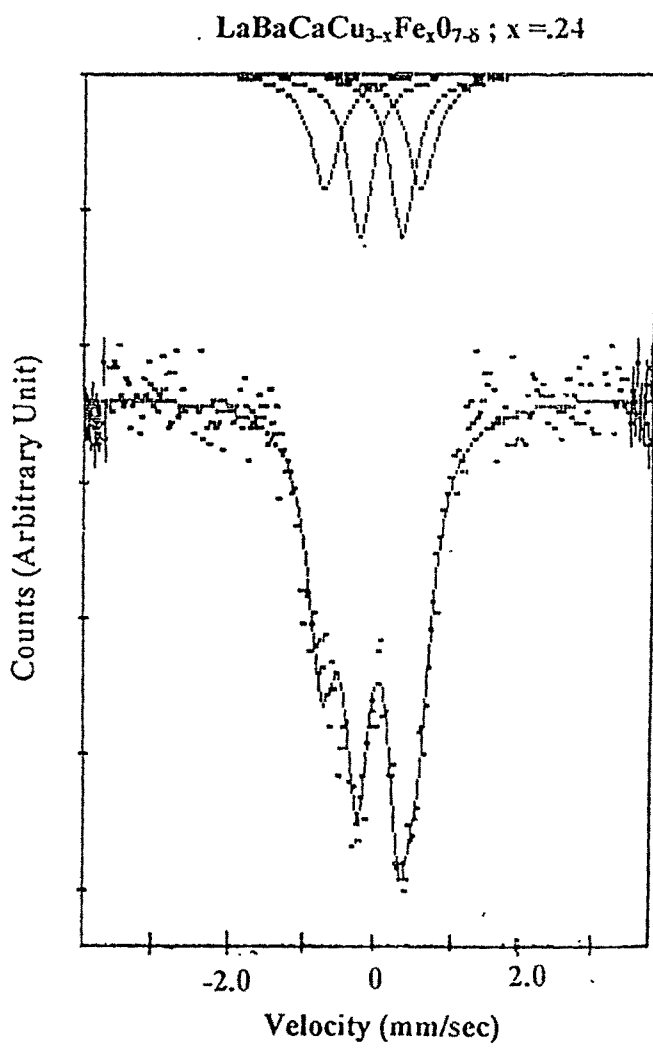


Fig. 6.1.17



But in case of 1113 system even for Fe 1% concentration about 35 % of Fe goes to Cu(II) site even though the oxygen content in these systems are quite high (35 ). Hence in this system the role played by oxygen in site occupancy may not be similar to the YBCO system. As the concentration of Fe increases more and more Fe goes to Cu(II) site. It should be noted that the value of  $T_c$  in case of Fe doped as well as Zn doped 1113 decreases but there is a drastic effect in case of Fe doping than Zn doping (35,42). This high percentage occupancy of Fe in Cu(II) site seems to be the reason for sharp reduction of  $T_c$  in these systems.

**References:**

1. J.G. Bednortz and K.A. Muller, *Z. Physik*, B64, 1986, 189.
2. H. Takayo, S. Uchida, K. Kilazawa and S. Tanaka, *Jap. J. Appl. Phys.*, 26, 1987, 123.
3. M.K. Wu, J.R. Ashbern, C.J. Torng, P.H. Hor, R.L. Peng, L. Gao, Z.J. Hung, Y.Q. Wang and C.W. Chu, *Phys. Rev. Lett.*, 58, 1987, 908.
4. H. Maeda, Y. Tanaka, M. Fukutomi and T. Asano, *Jap. J. Appl. Phys.*, 27, 1988, 209.
5. S.B. Quadri, L.E. Toth, M. Osofsky, S. Lawrence, D.U. Gabser and S.A. Wolf, *Phys. Rev.*, B35, 7235, 1987; G.R. Wagner, A.J. Panson and A.I. Brginski, *Phys. Rev.*, B36, 7124, 1987.
6. Yoshimi Kubo, Tsutomu Yoshitake, Junji Tabuchi, Yukinobu Nakabayashi, Atushi Ochi, Kazauki Utsumi, Hitoshi Igarashi and Masatomo Yonezawa : *Jap. J. Appl. Phys.*, 26, 768, 1987.
7. B.D. Dunlap, M. Slaski, D.G. Hinks, L. Soderholm, M.A. Beno, K. Zhang, C.U. Segre, G.W. Crabtree, W.K. Kwok, S.K. Malik, I.K. Schuller, J.D. Jorgensen and Z. Sungalia, *J. Mag. Mag. Mater*, 68, L139, 1987.
8. C.V. Tomy, R. Prasad, N.C. Soni and S.K. Malik, *Physics C*, 153-155, 174, 1988.
9. L. Forro, M. Raki, C. Ayache, P.C.E. Stamp, J.Y. Henry and J. Rossat-Mignod, *Physica C*, 153-155, 1357, 1988.

10. C.Uher and A.B. Kaiser, *Phys. Rev. B*36, 5680, 1987.
11. H.J. Trodahl and A. Mawdsley, *Phys. Rev. B*36, 8881, 1987.
12. Z. Henkie, R. Horyn, Z. Bukowski, P.J. Markowski and J. Klamut, *Solid State Commun.* 64, 1285, 1987.
13. R.S. Liu, J.R. Cooper, J.W. Loram, W. Zhou, W. Lo, P.P. Edwards and W.Y. Ling, *Solid State Commun.*, 86, 334, 1990.
14. E.M. McCarron III, M.K. Crawford and J.B. Paraise, *J. Solid State Chem*, 78, 192, 1989.
15. V.P.S. Awana and A.V. Narlikar, *Phys. Rev.*, B49, 9, 6353, 1994.
16. V.P.S. Awana, Ashwin Tulapurkar and S.K. Malik, *Phys. Rev.*, B50, 1994.
17. R.G. Buckley, D.M. Pook, J.L. Tellon, M.R. Persland, N.E. Flower, M.P. Staines, H.L. Johnson, M. Meylon, G.V. M. Williams and M. Wowden, *Physica C*, 174, 383, 1993.
18. J.L. Tellon and N.E. Flower, *Physica C*, 204, 237, 1993.
19. R. Nagarajan, Vikram Parate and C.N. Rao, *Solid State Commun.*, 84, 183, 1993.
20. T. Wada, A. Adachi, T. Mihara and R. Inaba, *Jpn. J. Appl. Phys.*, 27, L706, 1988.
21. A. One, T. Tanaka, H. Nozari and Y. Ishizawa, *Jpn. J. Appl. Phys.*, 26, L1687, 1987.
22. B. Jayaram, S.K. Agarwal, A. Gupta and A.V. Narlikar, *Solid State Commun.*, 63, 713, 1987.

23. H. M. Sung, J.H. Kung, J.M. Liang, R.S. Liu, Y.C. Chen, P.T. Wu and L.J. Chen, *Physica C*, 153-155, 866, 1988.
24. T. Saito, T. Noji, A. Endo, N. Higuchi, K. Fijimoto, T. Oikawa, A. Hattori and K. Funose, *Physica*, 148B, 336, 1987.
25. I. Felner, M. Kowitt, Y. Lehavi, L. BenDor, Y. Wolfus, B. Barbara and I. Nowik, *Physica C*, 153-155, 898, 1988.
26. J.M. Tarascon, P. Barboise, P.F. Miali, L.H. Greene, G.W. Hull, M. Eibschutz and S.A. Sunshine, *Phys. Rev.*, B37, 7458, 1988.
27. Y. Macuo, T. Tomita, M. Kyogoku, S. Awaji, Y. Aoki, K. Hoshino, A. Minanai and T. Fujita, *Nature*, 328, 512, 1987.
28. Giag Ziao, M.Z. Ciplak, A. Gavrin, F.H. Streitz, A. Bakshai and C.L. Chien, *Phys. Rev. Lett.*, 60, 1446, 1988.
29. H. Rajagopal, A. Sequeira, R. Gunshekaran, J.V. Yakhmi, I.K. Gopalkrishnan and R.M. Iyer, "Proc. Int. Conf. On Neutron Scattering", Bombay, 1991, *Physica*, B174, 372, 1991.
30. W.T. Fu, H.W. Zandbergen, C.J. Van Der Beek and L.J. DeJongh, *Physica C*, 156, 133, 1988.
31. A.H. Carim, A.F. deJong and D.M. de Leeuw, *Phys. Rev.* B38, 7009, 1988.
32. J.L. Peng, P. Klavins and R.N. Shelton, *Phys. Rev.* B39, 9074, 1989.
33. K. Yamaya, T. Yagi and Y. Okajima, *Solid State Commun.*, 87, 1113, 1993.
34. M. Buchgeister, W. Hiller, S.M. Hosseini, K. Kopitzki and D. Wagener in *Transport properties of Superconductors*, Ed. Robert Nicosky, World

- Scientific, Singapore 1990; G. Kallias, I. Panagiotopoulos, D. Niarches and A. Kostikas, *Phys. Rev.*, B48, 15995, 1993.
35. V.P.S. Awana, Rajvir Singh, D.A. Landinez, J.M. Ferreira, J. Albino Aguiar, A.V. Narlikar, *Physica C*, 277, 265-270, 1997.
36. A.I. Nazzal, V.Y. Lee, E.M. Engler, R.D. Jacowitz, Y. Tokura and J.B. Torrance, *Physica C*, 153, 1367, 1988.
37. N.V. Patel, M. Sarkar, P.K. Mehta and D.R.S. Somayajulu, *Solid State Physics, (India)*, 37C, 360, 1994.
38. R. Suryanarayanan, L. Ouhammu, Mamidanna, S.R. Rao, O. Gorochoy, P.K. Mukopadhyay and H. Pankowska, *Solid State Commun.*, 81, 7, 593, 1992.
39. B.W. Veal, W.K. Kwok, A. Umezawa, G.W. Crabtree, J.D. Jorgensen, J.W. Downey, L.J. Nowicki, A.W. Mitchell, A.P. Paulikas and C.H. Sowers, *Appl. Phys. Lett.*, 51, 279, 1987.
40. Rajni Bhauguna, R. Ganguly, H. Rajagopal, J.V. Yakhmi, A. Sequeira and B.A. Dasannacharya, *Solid State Physics (India)*, 37C, 339, 1994.
41. Rajvir Singh, R. Lal, U.C. Upreti, D.K. Suri and A.V. Narlikar, *Phys. Rev. B*, Vol. 55, No.2, 1216, 1997.